LABORATORY DEMONSTRATION MODEL ACTIVE CLEANING TECHNIQUE DEVICE

FINAL REPORT

D180-18031-1
MARCH 1974
CONTRACT NAS8-28270

Prepared for
George C. Marshall Space Flight Center
Marshall Space Flight Center
Alabama 35812

By
Boeing Aerospace Company
Research & Engineering Division
Seattle, Washington 98124

A Division of The Boeing Company

LABORATORY DEMONSTRATION MODEL
ACTIVE CLEANING TECHNIQUE DEVICE
FINAL REPORT

D180-18031-1

March 1974

by

R. L. Shannon

and

R. B. Gillette

Prepared Under Contract NAS8-28270

by

BOEING AEROSPACE COMPANY

Research and Engineering Division

Seattle, Washington 98124

(A Division of The Boeing Company)

for

George C. Marshall Space Flight Center

Marshall Space Flight Center, Alabama 35812

I

ACKNOWLEDGEMENTS

The authors are grateful to the following persons for their assistance in developing the laboratory demonstration model device:

Mr. Dale Watkins: Consultation on design problems. Design and fabrication of main power/plasma discharge sensor system. Assembly of control console and fabrication of RF electrode assembly.

Mr. Czeslaw Deminet: Design and fabrication of quartz plasma tubes and light pipes.

TABLE OF CONTENTS

1.0 SUMMARY

This report describes the work accomplished under the development phase of NASA Contract NAS8-28270. The objective of this program was to develop a laboratory demonstration model (LDM) of an active cleaning technique (ACT) device for space use. The principle of this device is based primarily on the technique for removing contaminants from optical surfaces which was developed under NASA Contract NAS8-26385. This technique utilizes exposure to a plasma to remove contaminants from a surface. The laboratory demonstration model incorporates both plasma cleaning and ion sputtering modes of operation.

During the design study phase of the present program a prototype device was developed and a preliminary design was established based on tests of the prototype device. One major problem remained unsolved after completion of the design study phase. The plasma tube development was based on the earlier assumption that plasma cleaning was caused by atomic oxygen reacting with the contaminant to form volatile products. This assumption proved to be erroneous since the plasma tubes, developed for operation at high vacuum ($<10^{-5}$ torr) conditions, produced atomic oxygen but did not produce measurable contaminant cleaning. Plasma cleaning under the companion contract (NAS8-26385) was accomplished at relatively high chamber pressures (10^{-3} to 10^{-2} torr) which resulted in a plasma discharge throughout the vacuum chamber.

Since the problem of producing active cleaning species at high vacuum ($<10^{-5}$ torr) conditions remained unsolved after completion of the design study phase, a major effort of the present program was to develop a suitable plasma tube for the laboratory demonstration model. After considerable experimental effort a plasma tube was developed which provides the active cleaning species at high vacuum conditions. It was shown that plasma cleaning occurs in the region of a visible plume which extends from the end of the plasma tube.

With the exception of the plasma tube, only minor modifications to the laboratory demonstration model design were required. The ACT device consists of a control console, cable bundles, plasma generator enclosure (which houses the plasma tube assembly), and an ion accelerator. The device can be operated at gas flow rates of 0.03 to 0.5 std cc/min and RF power inputs of 5 to 25 watts. The ion accelerator voltage can be varied from 1-3 KV in the sputtering mode of operation. Tests in the plasma cleaning mode show that carbon can be removed at a rate of 5×10^{13} to 3×10^{14} atoms/cm^2-sec 5-cm away from the plasma tube. In the ion sputtering mode, ion fluxes of 10^{13}-10^{14} ions/cm^2-sec are achieved 5-cm away from the accelerator.

2.0 INTRODUCTION

Spacecraft contamination problems have shown the need for developing an in-situ or active cleaning technique (ACT) for use in both space and vacuum chambers. Manned spacecraft contamination problems include deposition of volatile organic compounds onto windows, and light scattering from particulate contaminants surrounding the spacecraft. Sources of this contamination include outgassing of organic compounds, waste and water dumps, rocket plumes, and leakage from the life support system. Contaminant film deposition also occurs on unmanned spacecraft. This has been verified with quartz-crystal thin film monitors on Skylab (Reference 1) and on OGO-6 (Reference 2). A review of the spacecraft contamination problem has been published in Reference 3. Contamination can also occur during spacecraft testing in high vacuum chambers. For example, a film of back-streamed diffusion pump oil was apparently deposited on surfaces during thermal/vacuum testing of the extreme-UV spectroheliometer experiment for the Apollo Telescope Mount (ATM) vehicle (Reference 4). Another example of contaminant film deposition during environmental testing is discussed in Reference 5. In this case an extremely stable organic film was deposited onto telescope mirror surfaces during irradiation with low energy protons in a relatively clean vacuum environment.

Based on existing knowledge, contamination problems anticipated for future spacecraft include: (1) deposition of non-volatile substances onto optical components, sensing elements, and temperature control surfaces; (2) particulate and gaseous contamination near the spacecraft (resulting in light scattering and absorption); and (3) chemical contamination which can interface with upper atmosphere studies, analysis of interplanetary or planetary matter, and material processing experiments. Even though contamination effects can be reduced by changes in design, materials and operating procedures, the use of more sensitive surfaces and longer term missions will probably offset these improvements. Consequently an ACT is needed for space use.

Experiments reported in Reference 5 showed that exposure to a plasma is an effective means of removing hydrocarbon contaminant films from optical surfaces in a vacuum. Based on these experimental results two NASA funded investigations were conducted. One program (NASA Contract NAS8-26385) was aimed at developing an ACT for removing contaminants from optical surfaces in space. This effort concentrated on establishing the feasibility of using plasma for in-situ cleaning. The results of this effort are reported in References 6 and 7. The other program (NASA Contract NAS8-28270) was aimed at developing a laboratory demonstration model of an ACT device which incorporates both plasma cleaning and ion sputtering. The design study phase of this development program is reported in Reference 8. The present report covers the completion of the development program and describes the resultant laboratory demonstration model (LDM) ACT device.

3.0 PLASMA TUBE DEVELOPMENT

3.1 Background

Figure 1 shows the plasma tube configuration used for most of the plasma cleaning experiments reported in References 6 and 7. This plasma tube consisted of a 10 mm I.D. outer quartz tube, a 4 mm I.D. inner quartz tube, and diametrically opposed tungsten wire electrodes in the annulus. A 13.6 MHz RF power supply was used to produce the plasma discharge in the inner tube. A nominal pressure of about 4 torr (upstream of the plasma tube) was required for the discharge to be maintained. This resulted in an oxygen flow rate of about 50 std cc/min and a vacuum chamber pressure of 10^{-3} to 10^{-2} torr. Under these conditions there was a plasma discharge throughout the vacuum chamber in addition to that in the plasma tube. During these early cleaning experiments it was assumed that atomic oxygen was responsible for the plasma cleaning effects.

The development of an LDM ACT device required plasma tube operating conditions compatible with the NASA LDM test facility. The proposed NASA test facility used a 400 liter/sec Varian noble ion pump. This limited the oxygen flow rate to 0.18 std cc/min at a maximum vacuum chamber pressure of 10^{-5} torr. During the design study phase of the present contract (NAS8-28270) a plasma tube configuration was developed which would allow operation at low flow rates while supplying atomic oxygen to a surface at high vacuum conditions. Figure 2 shows this plasma tube configuration. The plasma tube pressure and gas flow rate are controlled by the flow restriction (capillary) at the downstream end of the tube. The capillary sizing was based on consideration of atomic oxygen recombination on the capillary wall in addition to flow rate and pressure considerations. Experimental results showed that this plasma tube configuration produced atomic oxygen. However, no plasma cleaning effects were produced. Consequently, it was concluded that the active cleaning species (not atomic oxygen) were destroyed by wall collisions during passage through the capillary. The details of this investigation are reported in Reference 8.

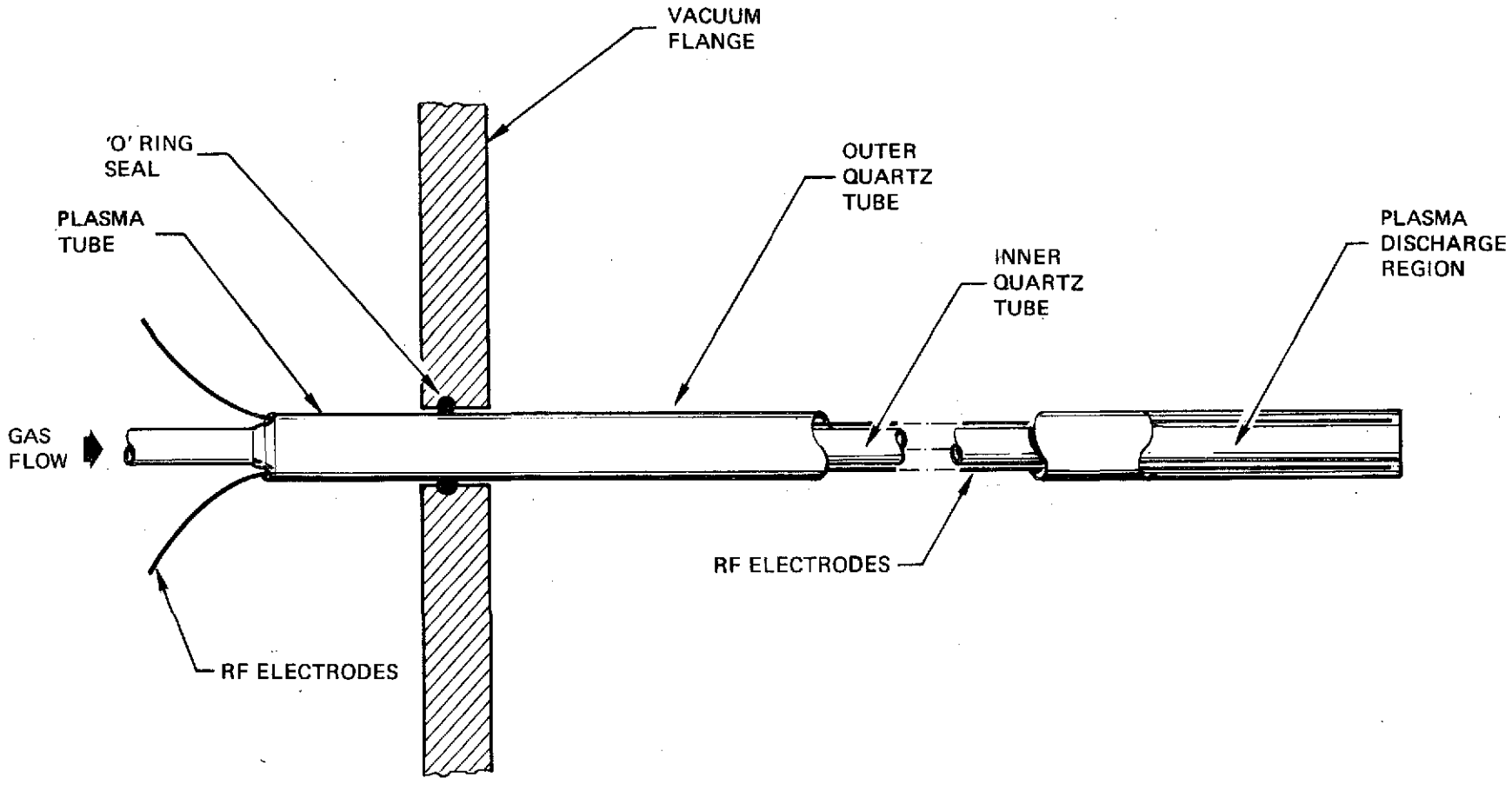

Figure 1: PLASMA TUBE CONFIGURATION USED FOR CONTRACT NAS8-26385

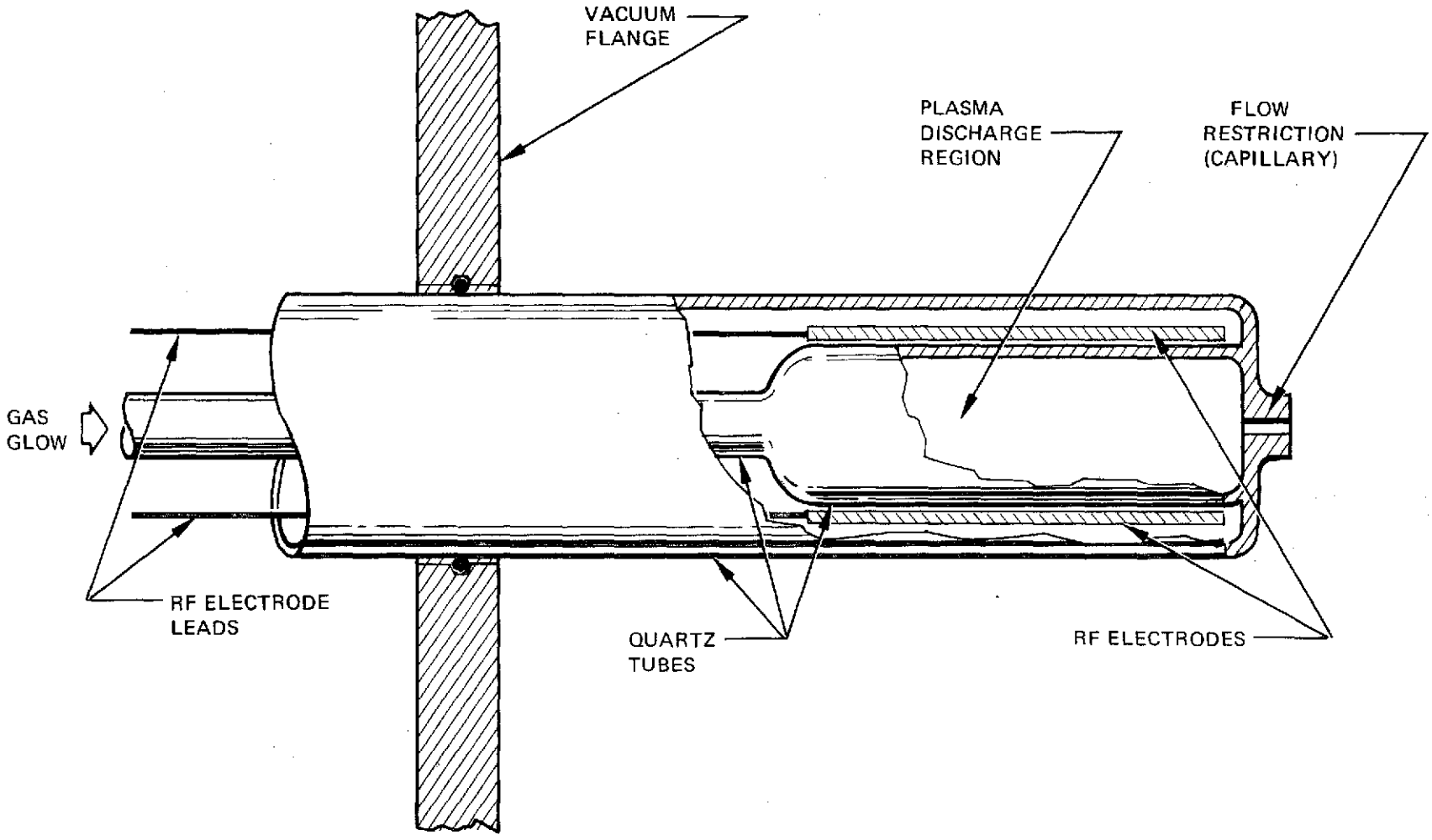

Figure 2: PLASMA TUBE CONFIGURATION USED IN DESIGN STUDY PHASE

3.2 Further Development Experiments

Since the plasma tube configuration developed during the design study phase did not produce the active cleaning species at low chamber pressures, further development experiments were required. The initial experiments were aimed at determining: (1) the feasibility of establishing a DC discharge through the existing plasma-tube capillary; and (2) whether or not surface cleaning could be accomplished at low chamber pressures with an axial DC discharge. A plasma tube with a 0.1 cm dia. by 0.4 cm length capillary, fabricated during the design phase, was installed in the plasma cleaning facility with a grounded brass screen placed against the downstream end of the capillary. This screen was used as the anode, and a tungsten wire probe, located inside the plasma tube, was used as the cathode for a DC discharge Initial tests showed that a DC discharge could be established, and that a glow (similar to the 'ignited plume' phenomena observed in earlier experiments at higher chamber pressures) was present downstream of the capillary even at chamber pressures less than 10^{-4} torr. This glow suggested that the active cleaning species were present downstream of the capillary.

To determine whether cleaning could be accomplished with this mode of operation, cleaning experiments were conducted using a MgF_2/Al-coated mirror contaminated with polymerized butadiene. Tests with this sample showed increased reflectance degradation with successive plasma exposures. Post-test examination showed a diffuse spot, about 1.5 cm in diameter, on the mirror. Apparently some electrode material had been deposited on the sample. It was also found that the brass screen material had coated the quartz around the capillary. Consequently it was decided that a DC discharge would be unsuited for the ACT device.

Experiments were then conducted to determine: (1) the feasibility of establishing an RF axial discharge through the existing plasma tube capillary; and (2) whether or not surface cleaning could be accomplished at low chamber pressures with an RF axial discharge. The plasma tube used in the DC discharge tests was installed in the test chamber with a grounded molybdenum electrode located in the downstream end of the capillary. Several RF electrode

configurations were evaluated including: (1) a wire probe in contact with the plasma gas upstream of the capillary; (2) same as item (1) except protected with a glass sheath; and (3) parallel plate electrodes located outside the plasma tube upstream of the capillary. Results of these tests showed that a satisfactory axial discharge in the capillary could only be produced using RF applied to both a wire probe in the plasma and parallel plate electrodes. Operation with this arrangement provided a visible gas plume in the vacuum chamber at pressures as low as 5×10^{-5} torr. Furthermore the axial discharge could be sustained over a range of pressures and RF power levels. Both molybdenum and tungsten wire probes were evaluated, with the former providing the most satisfactory results from the standpoint of minimizing contamination on the walls of the plasma discharge tube.

To determine whether cleaning could be accomplished with the axial RF discharge, a MgF_2/Al-coated mirror was installed in the chamber and coated with polymerized butadiene. Reflectance measurements were performed after various exposure periods in an oxygen plasma. Results showed that the diffuse appearance of the mirror, visible after contamination, gradually disappeared as the exposure time increased. Reflectance data showed a large increase in reflectance in the region less than about 230 nanometers (e.g., 28 to 64 percent at 120 nm), and a relatively small increase in the region longer than 230 nm (e.g., 56.5 to 63 at 250 nm). Post-test examination of the specimen revealed that the exposed area was slightly darker than the protected surface area, although both areas were highly specular. This suggests that electrode material may have been deposited on the specimen during exposure as the contaminant film was removed. An examination of the other apparatus showed that a dark coating was deposited on the plasma tube walls adjacent to the molybdenum wire electrode, and that the molybdenum aperture on the downstream end of the capillary showed no signs of sputtering. It was concluded from the test that plasma cleaning could be accomplished at low chamber pressures using an axial RF discharge. However, additional work was needed to develop a design wherein an axial discharge could be sustained without exposing electrodes to the plasma gas.

A plasma tube was then constructed which allowed experimentation with various electrode configurations outside the vacuum environment. This plasma tube configuration is shown in Figure 3. Tests with this tube showed that an axial RF discharge through the capillary and visible gas plume could be obtained with electrodes located outside the glass walls. Based on these results a plasma tube was built for the LDM ACT device (see Figure 4). However, operation of this tube failed to produce either a discharge through the capillary or a visible plume. These negative results may have been caused by: (1) adverse electric fields arising from the electrode leads; (2) the fact that the grounded chamber surrounded the plasma tube, whereas, in the tests outside the chamber the grounded chamber was downstream of the discharge region; or (3) the high vacuum conditions immediately downstream of the capillary, whereas, in tests outside the chamber the downstream pressure (in the 30 mm ID tube) would not be as low as the chamber pressure. The results of later plasma tube development tests indicate that item (1) was probably the cause of the negative results.

Tests were then conducted using a 4 mm ID quartz plasma tube with no capillary at the end and with external axial RF electrodes. The RF power was brought into the chamber through a separate feedthrough and the electrode leads were connected using soft solder. This configuration is shown in Figure 5. Results of these tests showed that: (1) an axial discharge and visible plume could be established; (2) the chamber pressure and flow rate could be maintained at the desirable low values; (3) the shape and position of the discharge were dependent on the gas flow (or plasma tube pressure) and the relative positions of ground and RF electrodes; and (4) the axial symmetry of the visible plume appeared to be dependent on the symmetry of fields produced by the electrodes.

Subsequent to the above experiments, a cleaning test was conducted using a carbon-coated quartz crystal microbalance (QCM). The QCM was mounted on a rod such that it could either be axially translated or be rotated through the visible plume. It was found that: (1) carbon removal occurred when the QCM was located in the visible plume; (2) carbon removal did not occur when located outside the visible plume; and (3) the cleaning rate decreased as distance between the QCM and plasma tube increased.

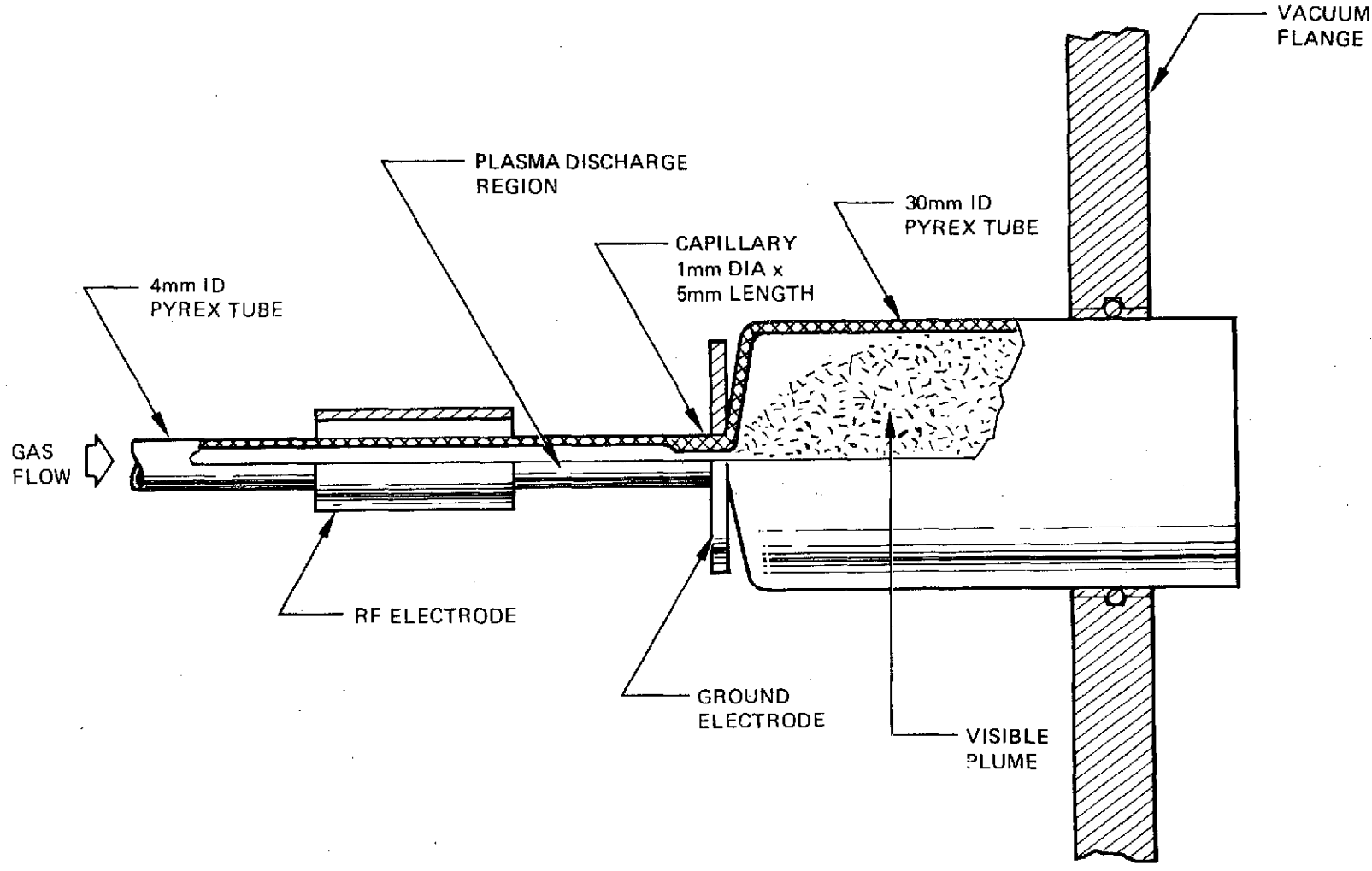

Figure 3: EXPERIMENTAL SETUP FOR AXIAL RF DISCHARGE

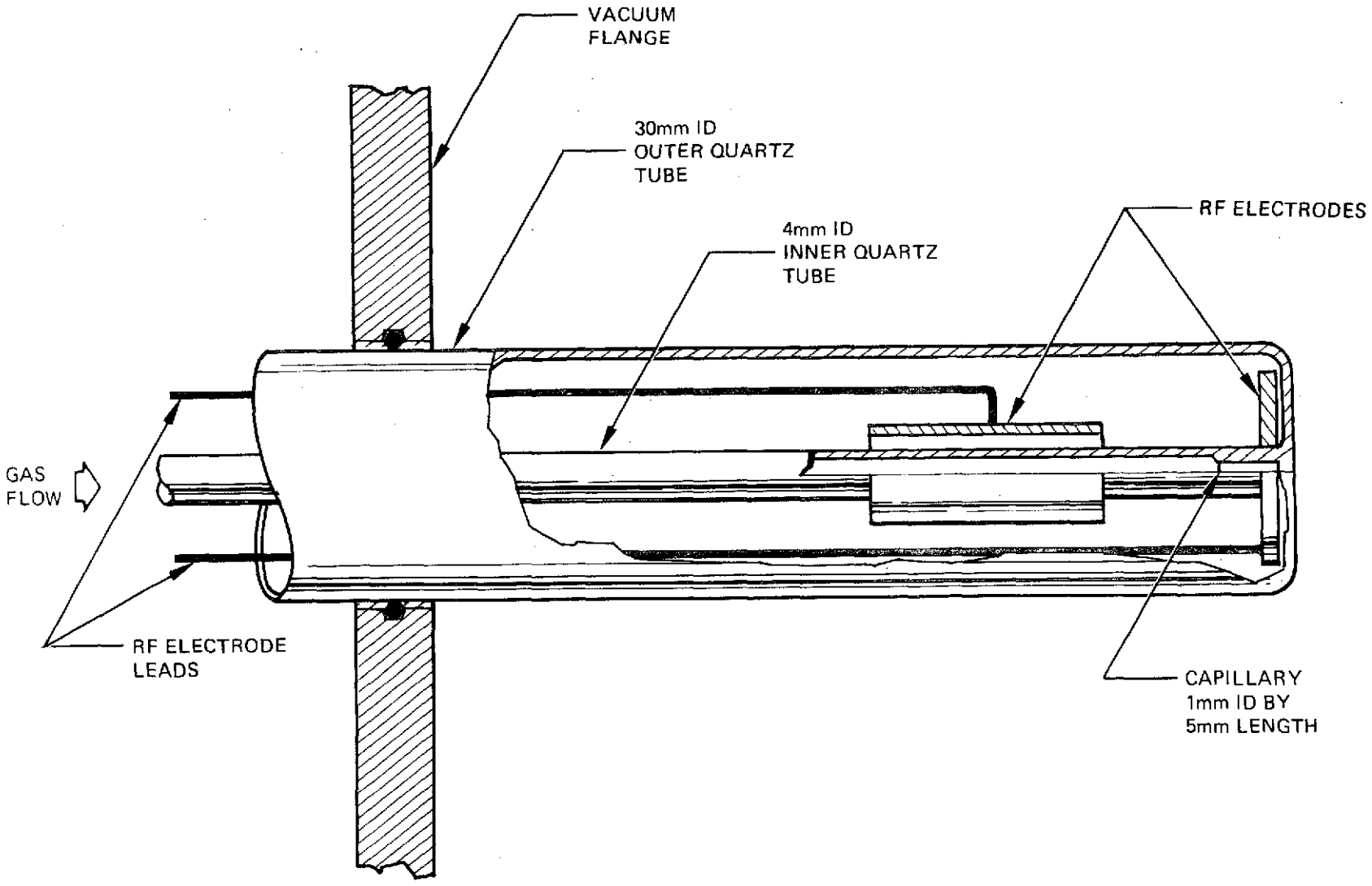

Figure 4: PLASMA TUBE CONFIGURATION FOR AXIAL DISCHARGE WITH CAPILLARY

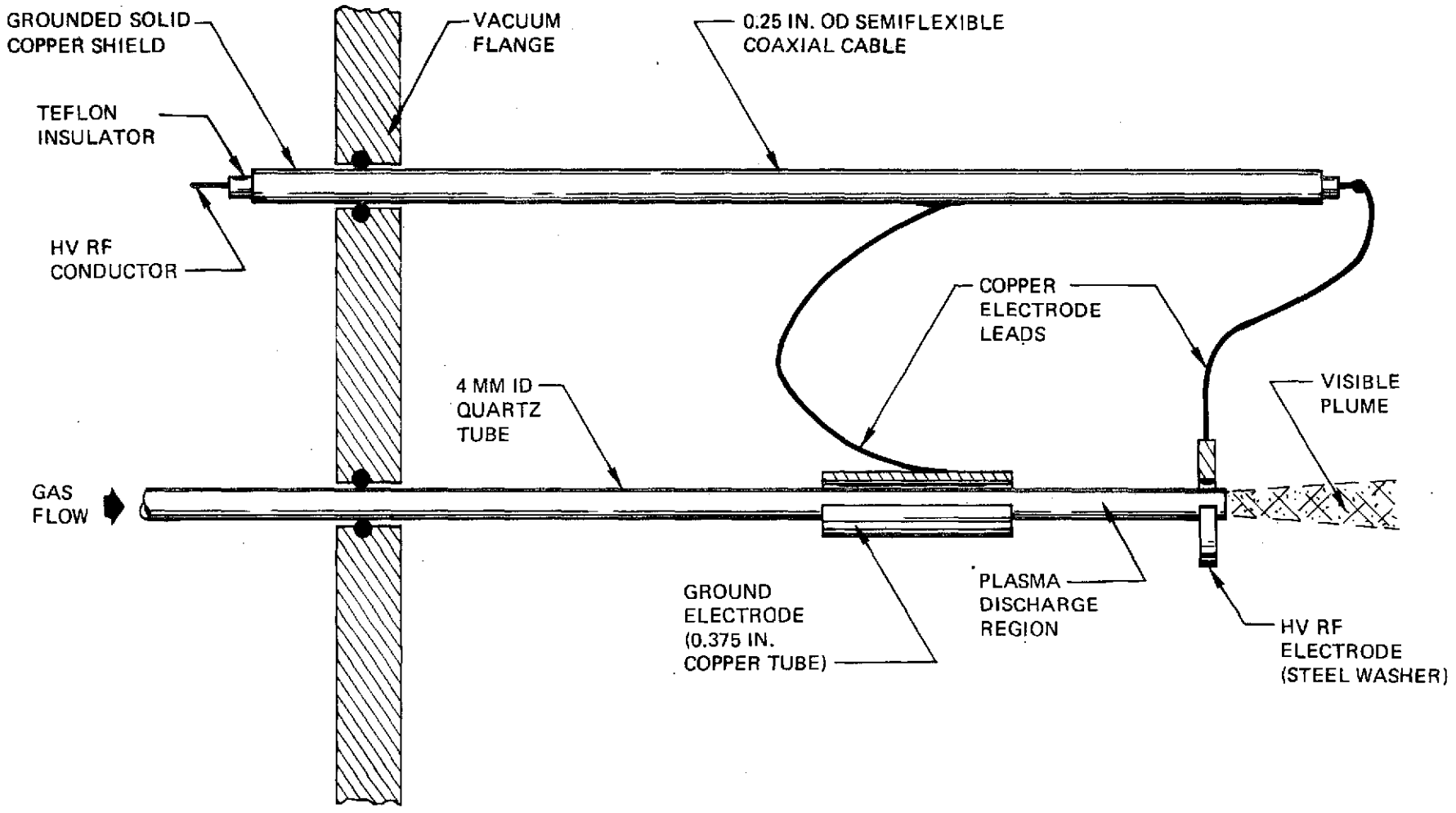

Figure 5: PROTOTYPE PLASMA TUBE CONFIGURATION

Further experiments using this plasma tube configuration (Figure 5) were made in conjunction with the companion contract NAS8-26385. Detailed results of these experiments are reported in Reference 7. In general, the results demonstrated that: (1) the plasma tube/electrode design allowed operation in a high vacuum environment; (2) electrodes could be located outside the quartz plasma tube walls, thus eliminating electrode contamination problems; and (3) the cleaning pattern produced is highly dependent on a number of variables, as discussed above.

3.3 LDM Plasma Tube Development

Further plasma tube development was required to establish a suitable design for the LDM ACT device. Successful operation of a single-wall quartz plasma tube (discussed above in Section 3.2) was achieved utilizing RF electrodes located in the high vacuum environment adjacent to the tube. Hence, lead-in conductors were not confined to the annular region between two quartz tubes as dictated by the ACT plasma tube design. Also the RF power requirements for this plasma tube were too large for the LDM ACT device.

The plasma tube configuration used in the development experiments consisted of a 4 mm ID inner quartz tube and a 30 mm ID outer quartz tube. Axial RF electrodes placed in the annulus consisted of a length of brass tubing as the upstream ground electrode, and a copper washer as the downstream 'high voltage' electrode. A semiflexible coaxial cable was used to conduct the RF power to the electrodes. The outer conductor was connected to the upstream ground electrode, and the inner conductor to the downstream RF electrode. Satisfactory operation of the plasma tube depends on the connection between the RF lead (inner conductor of coaxial cable) and the downstream electrode. Initially this connection was made with a wire that was routed as far away from the plasma discharge region (inner quartz tube) as possible. The asymmetry of this configuration caused difficulty in establishing a plasma discharge and a visible plume. Also the visible plume, when obtained, was deflected at an angle of about 45° to the plasma tube axis. Subsequently, the connection between the RF lead and downstream electrode was made with a cylindrical wire screen that extended over the plasma discharge region. This

configuration resulted in a symmetrical visible plume. Tests also showed that the plasma discharge and plume characteristics are dependent on the distance between the electrodes and the downstream end of the plasma tube. The establishment of a plasma discharge and a visible plume was also accomplished with the plasma tube installed inside the grounded RF shield tube as planned for the ACT device.

In an attempt to reduce the RF power requirements, experiments were conducted using various modifications to the impedance matching network. This network coupled the 13.6 MHz power supply to the plasma tube. Efficient RF coupling should allow a reduction in power requirements. The results of these experiments showed that, with the best coupling achieved, initiation of the plasma discharge required 100 watts at 13.6 MHz. The discharge could be sustained with 80 watts forward (30 watts reflected) power. From these results it was concluded that a relatively large amount of power (about 100 watts) is required for plasma discharge operation at a frequency of 13.6 MHz.

Since the plasma discharge occurs in the low pressure region at the downstream end of the plasma tube, it was reasoned that higher RF frequencies would produce a discharge at lower power inputs. Consequently, experiments were initiated using a 'Microdot Model 406A' power oscillator which has a 50-200 MHz frequency range. The initial experiments showed that the higher frequency discharge greatly improved the plasma tube performance. The visible plume was brighter and could be produced at very low plasma-tube flow rates (less than about 0.05 std cc/min). Instrumentation was not available to measure the power input but the maximum available from the Microdot power supply is on the order of 50 watts.

An improved electrode system was then developed which consisted of a series of metal disks centered along the plasma tube axis. The upstream disk was used as the ground electrode, and the downstream disk as the RF electrode. The remaining disks (two or three) were electrically insulated and equally spaced between the two electrodes. The purpose of these disks was to help provide a uniform axial field between the electrodes. A metal tube was attached to the ground electrode to shield the upstream region from the RF field. A coaxial cable was used to conduct the RF power to the electrodes. The shield

braid was connected to the ground electrode, and the insulated center conductor was routed axially through the ground electrode and insulated disks to the RF electrode. Another lead was similarly routed, but diametrically opposed, to provide symmetry of the electric field.

Experiments using the improved electrode configuration resulted in the following observations: (1) the production of a visible plasma plume is enhanced by having a discharge downstream of the RF electrode; (2) production of a visible plume is inhibited when a discharge occurs upstream of the electrode system; (3) extension of the tube attached to the upstream electrode inhibits the formation of an upstream discharge; (4) the effectiveness of the insulated disks, positioned between the electrodes, is uncertain; and (5) a visible plume could be produced with the RF shield tube in place over the plasma tube.

Based on experiments with the improved electrode system, a plasma tube/electrode system was designed for the LDM ACT device. This design is described in the following section.

3.4 LDM Plasma Tube Design

The LDM plasma tube was designed to provide adjustable electrode positions, RF shielding of the upstream gas, and light pipes to transmit the light from the plasma discharge to the outside of the plasma tube assembly. The basic design configuration is shown in Figure 6. Two disks are used for the electrodes. The upstream ground electrode is brazed to a tube which acts to shield the upstream gas from the RF field and provides the ground lead. The downstream RF electrode is connected to the RF power by means of two diametrically opposed leads. These leads are insulated by routing them through lengths of quartz tubing which pass through clearance holes in the ground electrode. Two light-pipes, made from quartz rod, are used to transmit light from the plasma discharge to the outside of the plasma tube. Diametrically opposed clearance holes in the electrodes allow the light pipes to be positioned to view either the region between the electrodes, or that downstream of the RF electrode. Figure 6 shows the light pipes positioned to view both regions. This plasma tube/electrode configuration allows independent adjustment of the distance between electrodes and the distance between the RF electrode and the downstream end of the plasma tube.

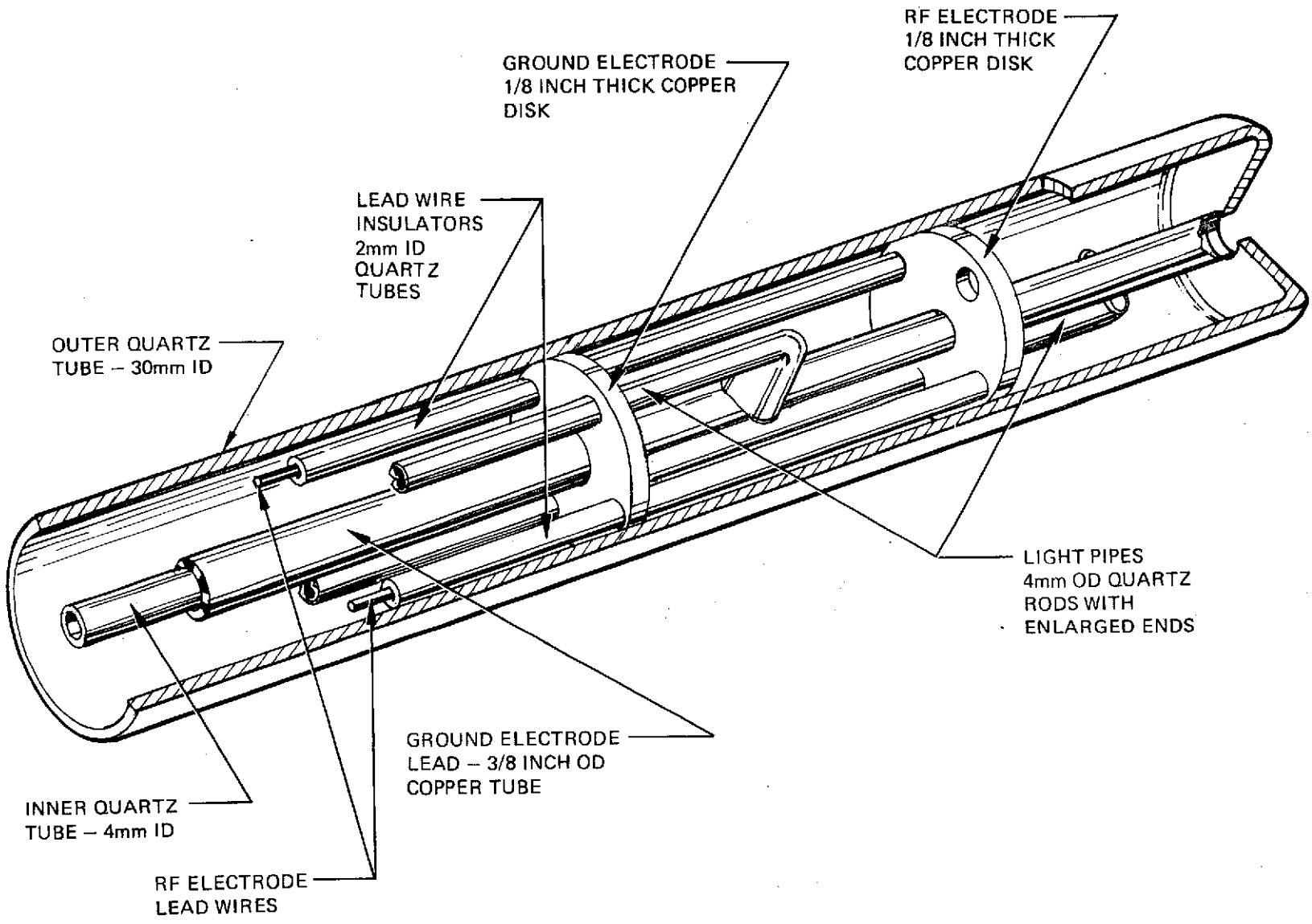

Figure 6: LDM PLASMA TUBE CONFIGURATION

Figure 7 shows a picture of the basic electrode assembly parts. The two light pipes, ground electrode assembly, RF electrode, RF leads and insulators are shown along with the RF connector block. The RF connector block is a split teflon block that clamps onto the RF lead insulators. This block has clearance holes for the ground electrode tube and the light pipes. Also seen in Figure 7 are the pin connectors which are brazed onto the ends of the RF leads and the threaded end of the disassembled RF lead which screws into the RF electrode. The completed basic electrode assembly is shown in Figure 8.

Figure 9 shows the remaining components of the plasma tube assembly. The RF connector assembly provides the connection between the semi-flexible coaxial cable center-conductor and the two RF leads. The copper clamping block and body provide the ground connection between the semi-flexible coaxial cable shield and the ground electrode tube. This clamping also fixes the relative electrode positions. Clearance holes are provided in the clamping block/body for the light pipes. The teflon retainer and spacer are used to mount the electrode assembly in the plasma tube which has a lip for this purpose.

Figure 10 shows the completed electrode assembly. Screws are used to fasten the RF connector block to the RF connector assembly. All of the copper parts in the electrode assembly were electroplated with gold to prevent corrosion and to enhance electrical conductance.

The complete plasma tube assembly is shown in Figure 11. All connections are made at the upstream end of the assembly. The RF power lead is connected to the semi-flexible coaxial cable, the gas supply line to the center quartz tube, and the light sensors to the exposed ends of the light pipes. The plasma tube assembly is shown mounted in the LDM vacuum flange in Figure 12. An '0' ring seal is used between the vacuum flange and the outside of the plasma tube.

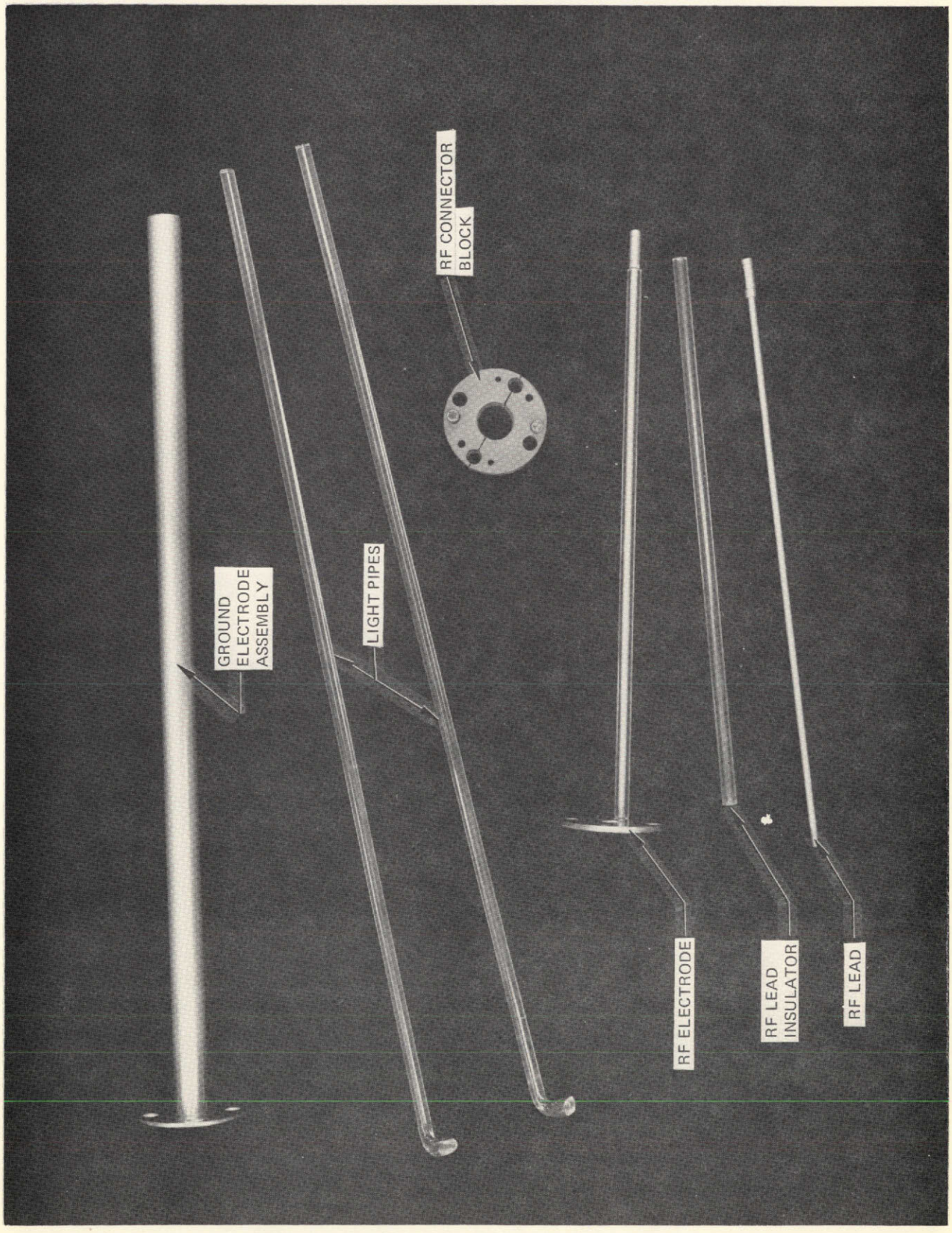

Figure 7: BASIC ELECTRODE ASSEMBLY PARTS

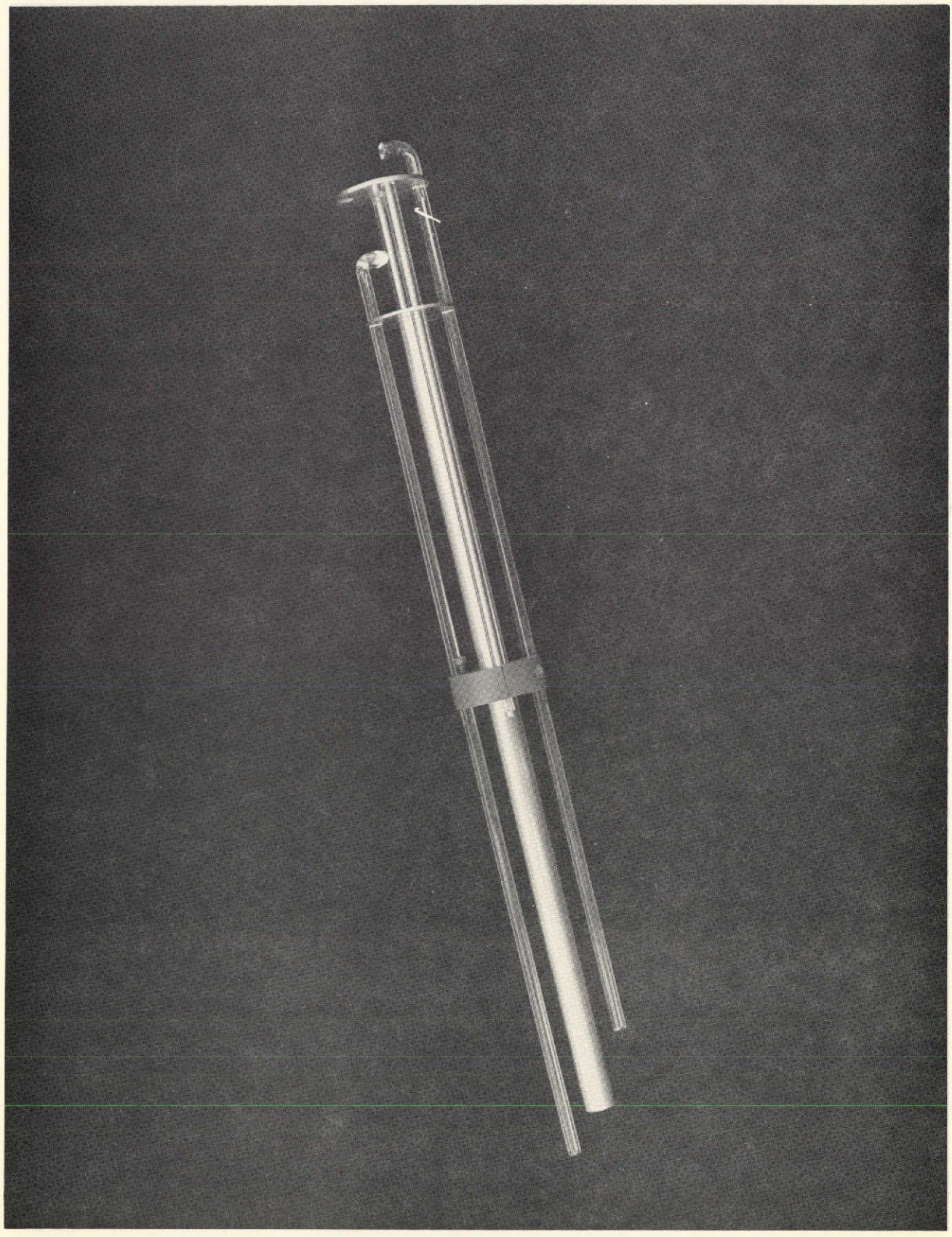

Figure 8: BASIC ELECTRODE ASSEMBLY

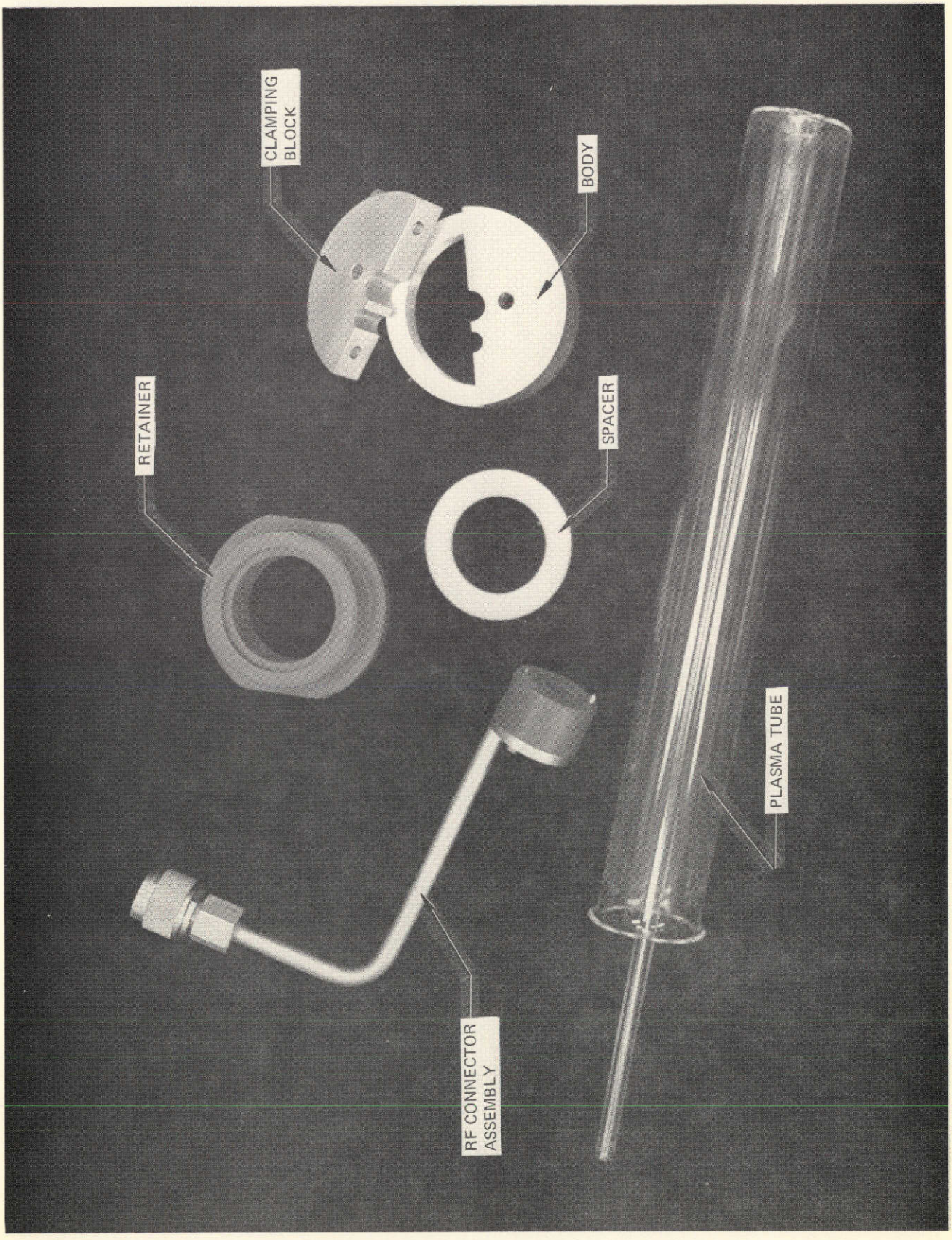

Figure 9: PLASMA TUBE ASSEMBLY COMPONENTS

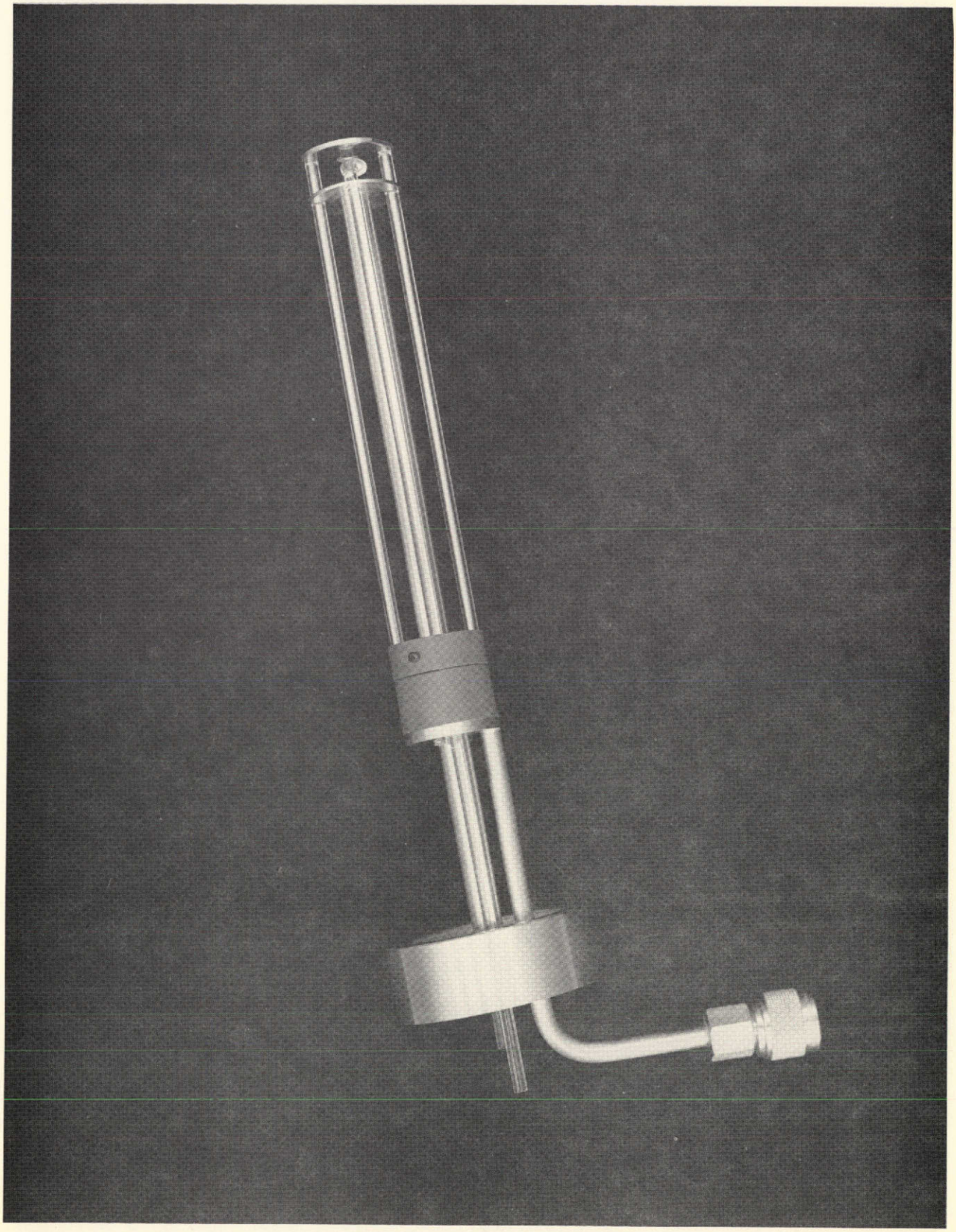

Figure 10: RF ELECTRODE ASSEMBLY

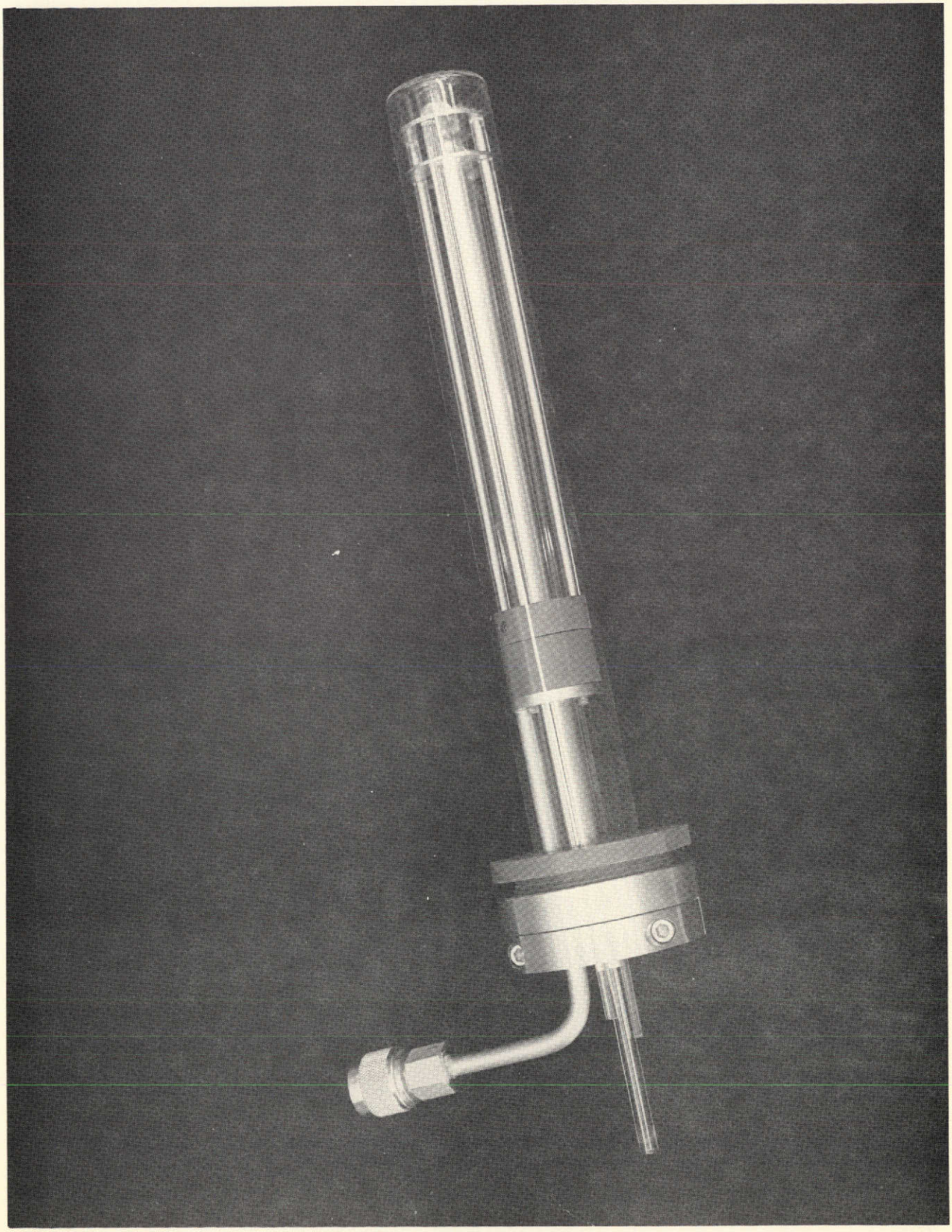

Figure 11: PLASMA TUBE ASSEMBLY

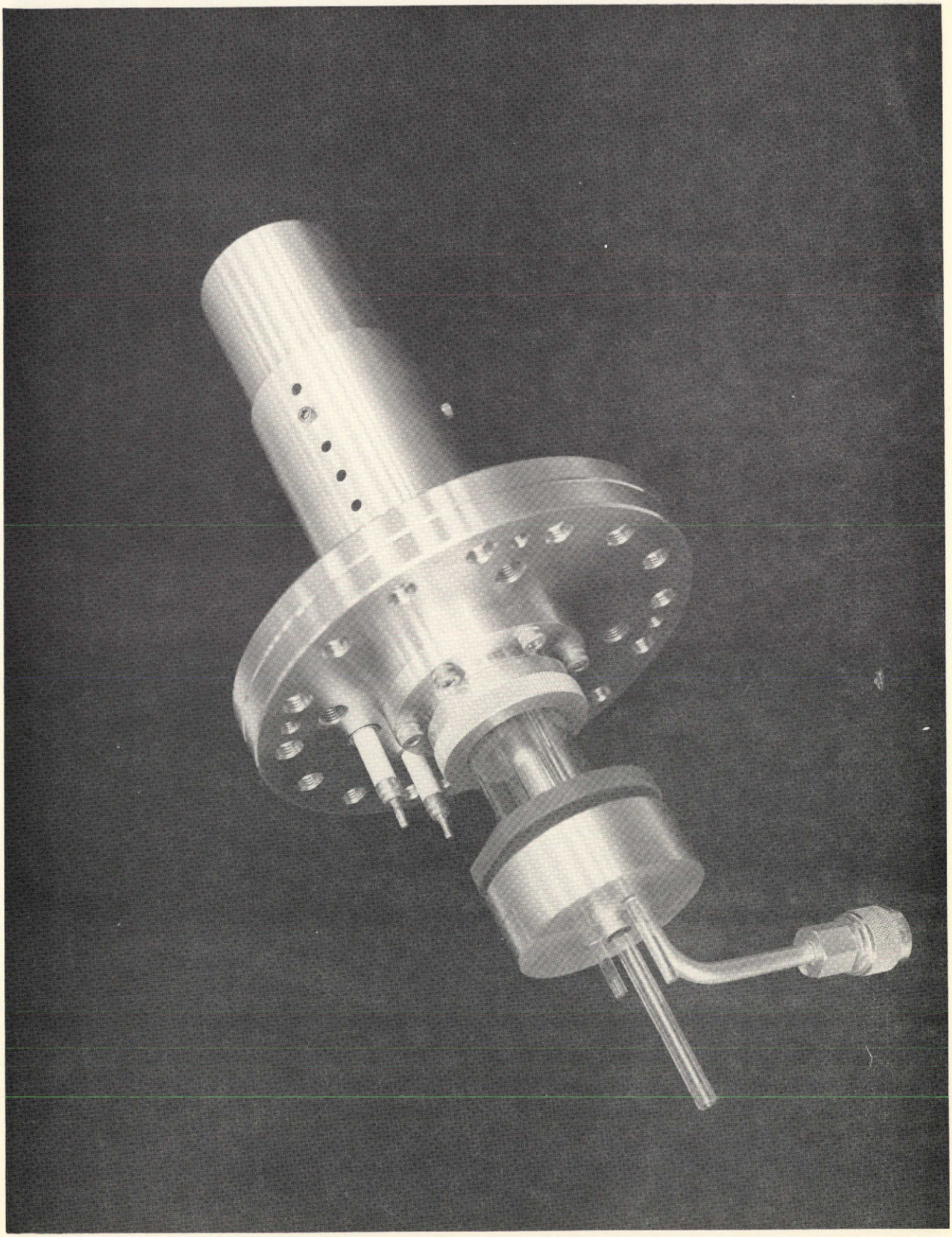

Figure 12: PLASMA TUBE ASSEMBLY INSTALLED IN VACUUM FLANGE

4.0 LDM ACT DEVICE DESIGN

4.1 General Description

The LDM ACT device consists of control console, cable bundles, plasma generator enclosure, plasma tube assembly, and ion accelerator assembly. The LDM design was based on the following specifications:

(1) The device was to be capable of operating in a plasma cleaning mode with an optional ion sputtering mode.

(2) Device must be compatible with operation in NASA test facility
   (a) Nominal oxygen flow rate of 0.18 std cc/min (based on 400 liter/sec Varian-type noble ion pump at 10^{-5} torr pressure).
   (b) Plasma generator enclosure must mount with Varian-type vacuum flange on a 6-inch (15.2 cm) diameter port.
   (c) RF shielding must be provided.

(3) Plasma generator enclosure must be capable of remote mounting inside a vacuum chamber.

(4) Plasma tube extension length must be adjustable from 9.7 to 17.3 cm with respect to mounting flange.

(5) Remote operation of device from a control console required.

The control console contains the gas supply, RF power generator, high voltage power supply, plasma discharge sensor meters, and gas supply and plasma tube pressure gauges. These components allow the LDM to be operated from the control console. A photograph of the control console is shown in Figure 13. Figure 14 shows an interior rear view of the control console. Connections to the control console are made at the bottom rear of the rack (see Figure 15).

The plasma generator enclosure houses the plasma tube assembly and provides the required RF shielding. The enclosure also houses the light sensors, Pirani vacuum gauge tube, and variable leak valve. A photograph of the plasma generator enclosure is shown in Figure 16. Connections are made to feedthrough fittings and access to the interior is provided by a hinged door. Figure 17 shows a photograph of the plasma generator enclosure with the ion accelerator attached to provide the optional ion sputtering mode of operation.

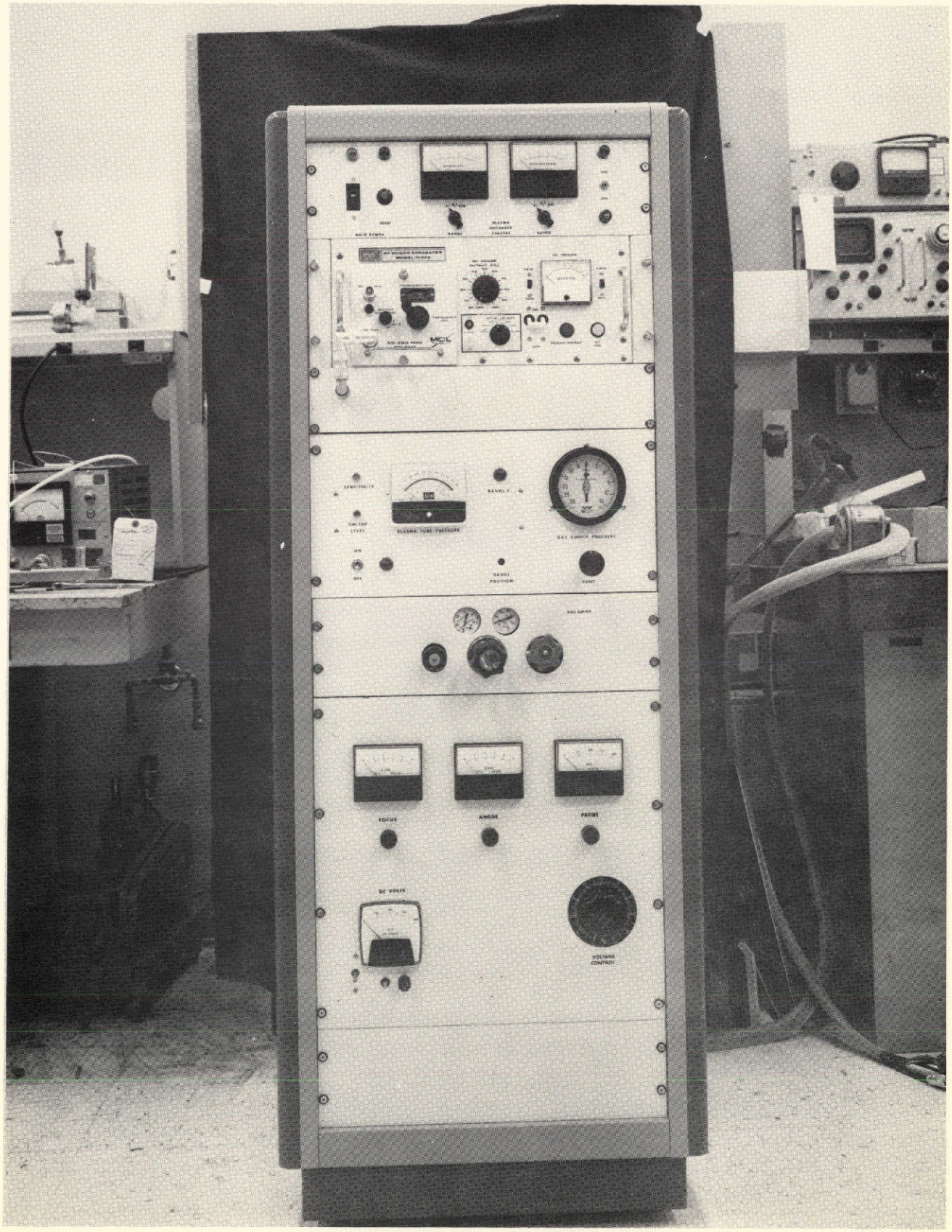

Figure 13: CONTROL CONSOLE

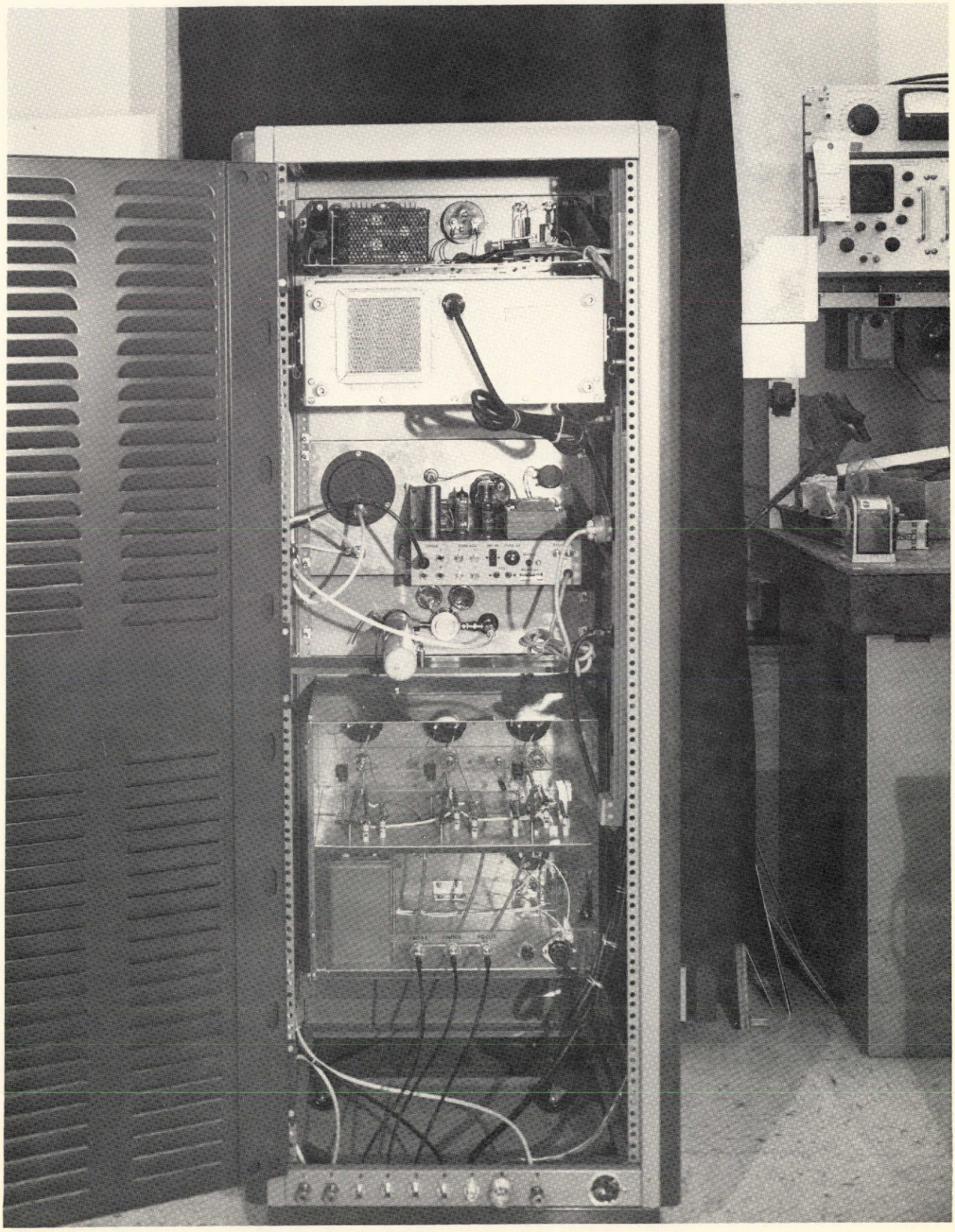

Figure 14: REAR INTERIOR VIEW OF CONTROL CONSOLE

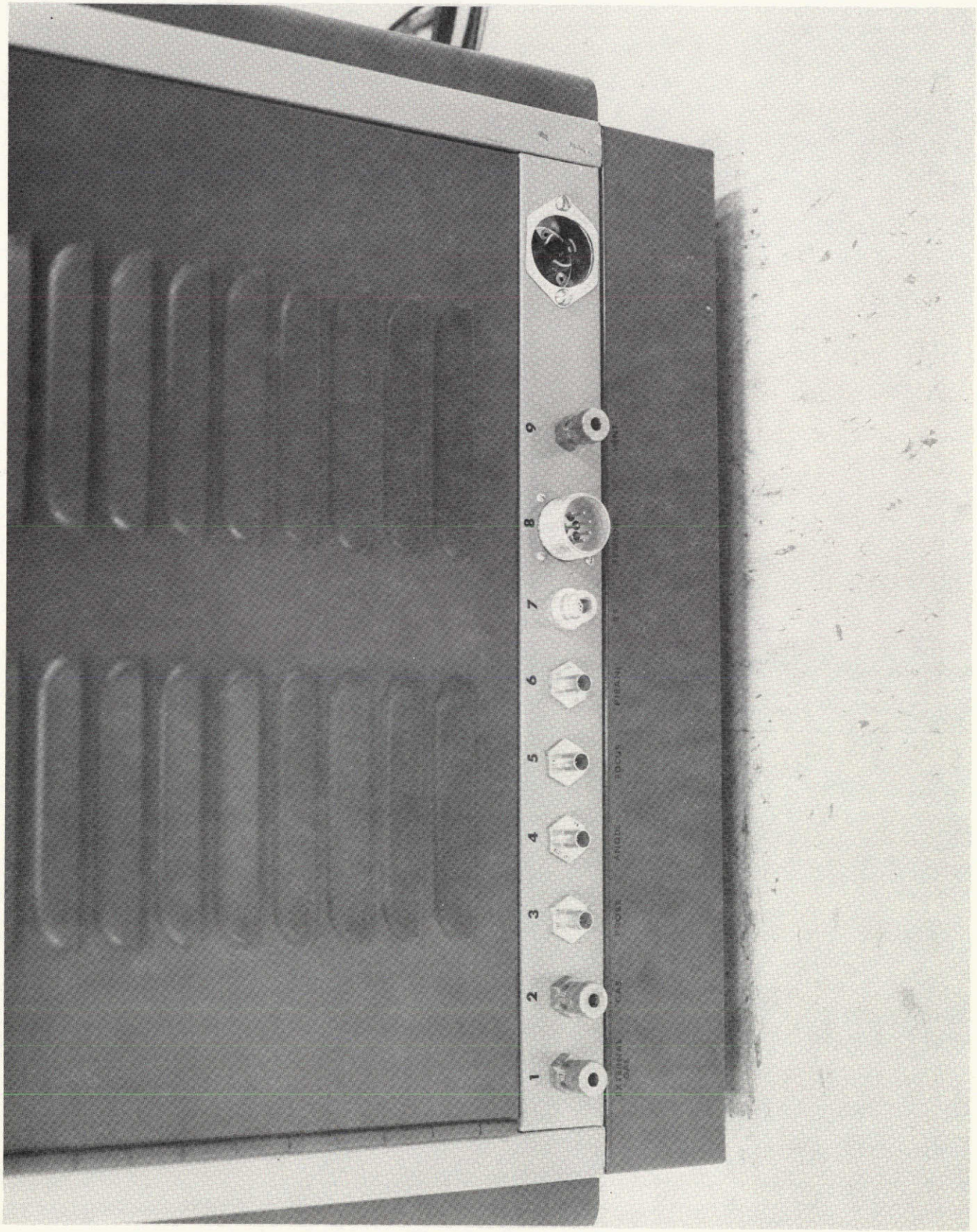

Figure 15: CONTROL CONSOLE CONNECTIONS

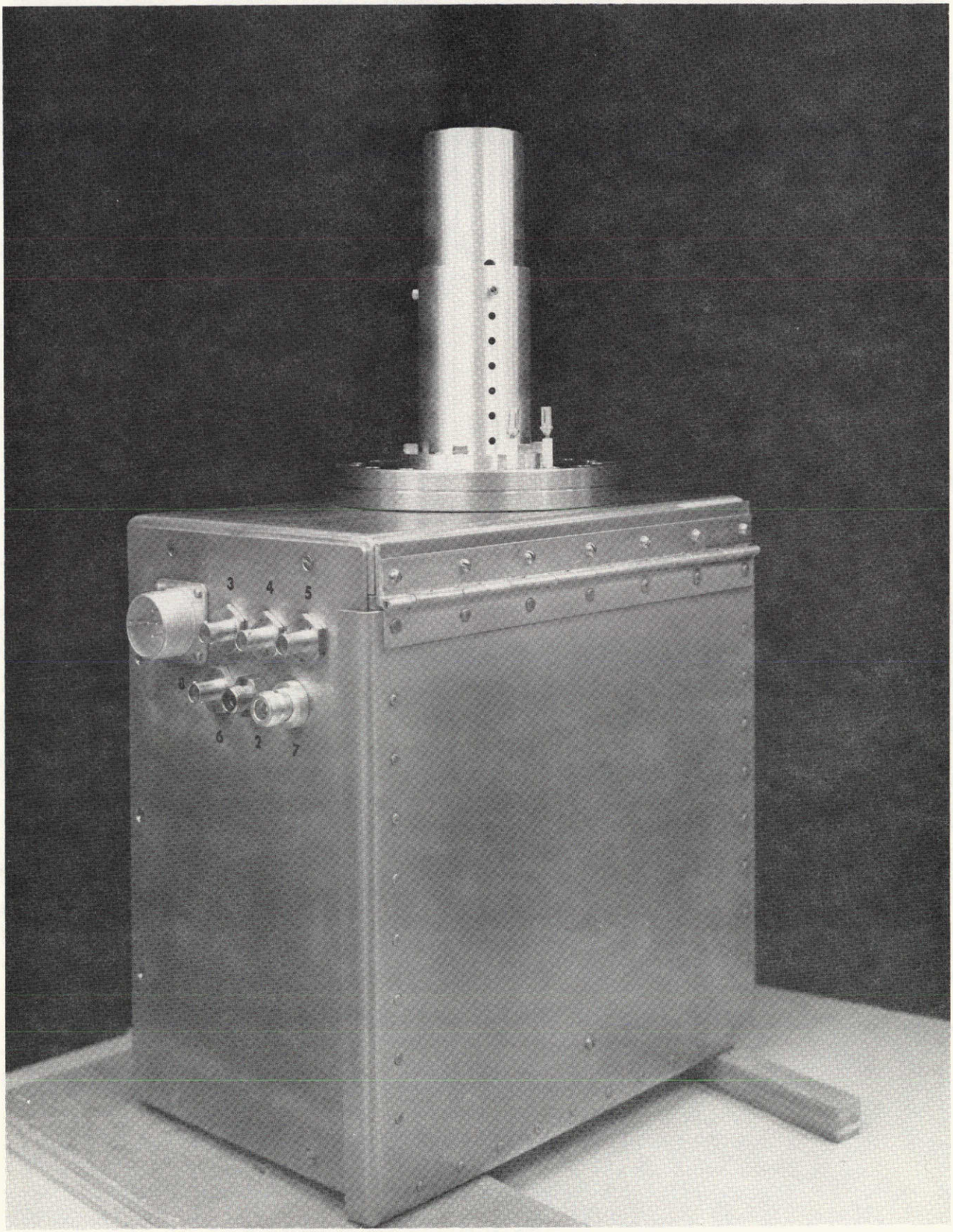

Figure 16: PLASMA GENERATOR ENCLOSURE

Figure 17: PLASMA GENERATOR ENCLOSURE WITH ION ACCELERATOR ATTACHED

Normally, a single cable bundle connects the control console to the plasma generator enclosure. However, the optional mounting of the plasma generator enclosure inside a vacuum chamber requires an additional cable bundle and a vacuum feedthrough flange. Figure 18 shows a photograph of this optional vacuum flange/cable bundle assembly. Both cable bundles are 12 feet (3.66 meters) in length.

A general gas/electrical diagram of the LDM ACT device is shown in Figure 19. The following sections describe the various systems depicted in this diagram.

4.2 Main Power/Plasma Discharge Sensors

The main power and plasma discharge sensor controls are located in the top panel of the control console. Figure 20 shows a close up view of this panel. The main power switch provides power to the plasma discharge sensor system directly and to the control console electrical plug-in-strip through an interlock relay/reset switch. As a safety feature, the relay may be reset only if the plasma generator enclosure door is closed (see Figure 19). The door switch may be seen in Figure 21 which shows an interior view of the plasma generator enclosure.

The plasma discharge sensors are light sensitive diode mounted on the ends of the plasma tube light pipes. The mounted light sensitive diode assemblies can be seen in Figures 21 and 22.

The plasma sensor power supply provides a fixed voltage across the light sensitive diodes and the plasma discharge intensity is indicated by the current flow through the ammeters (see Figure 19). These meters are labeled upstream and downstream intensity on the control console panel, and a range switch is provided for each meter (see Figure 20).

4.3 RF Power System

The RF power generator is pictured at the bottom of Figure 20. It is a commercial unit, manufactured by MCL Inc., of La Grange, Illinois, capable of generating 65 watts (or more) of power in the 50-200 MHz frequency range.

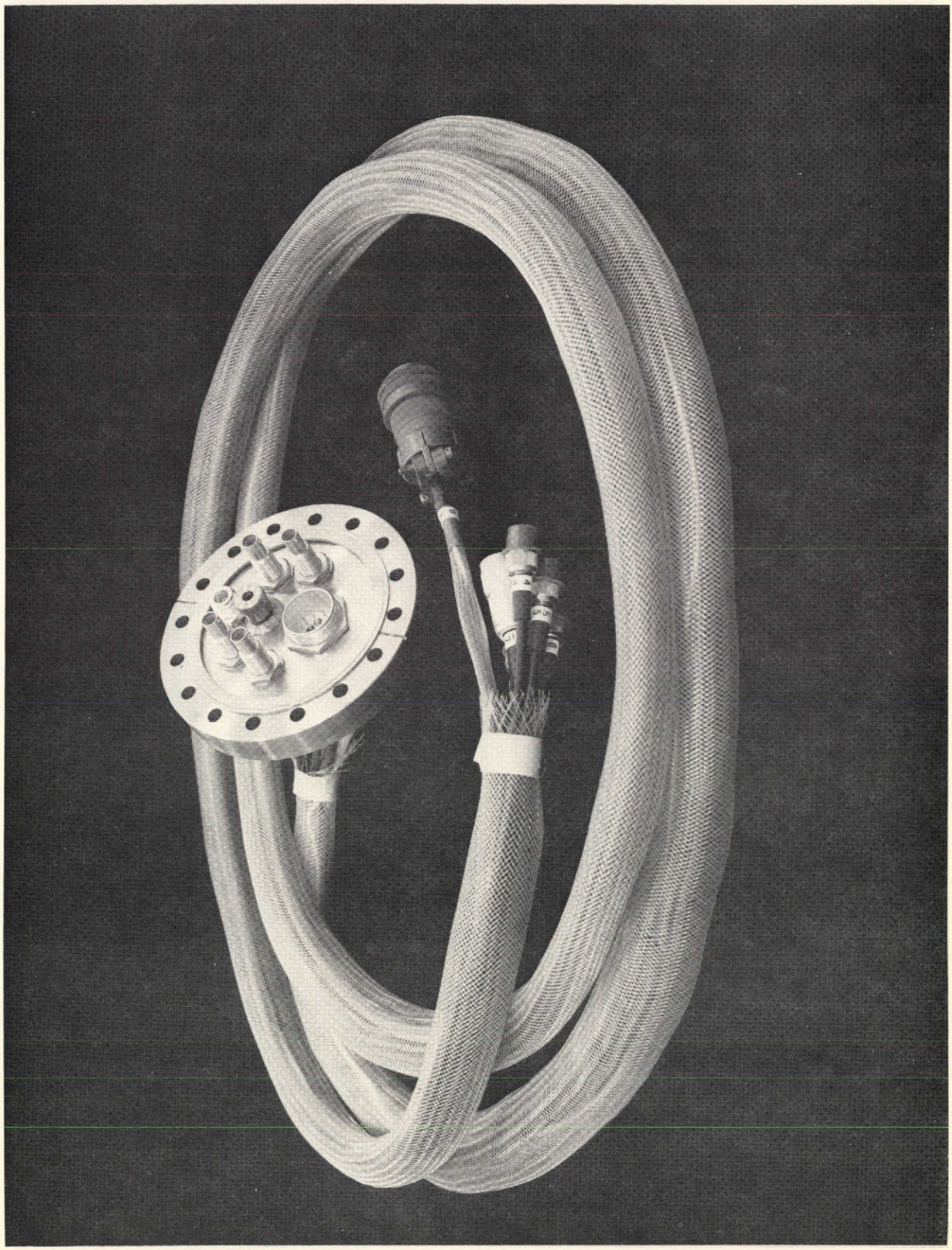

Figure 18: VACUUM FLANGE/CABLE BUNDLE ASSEMBLY

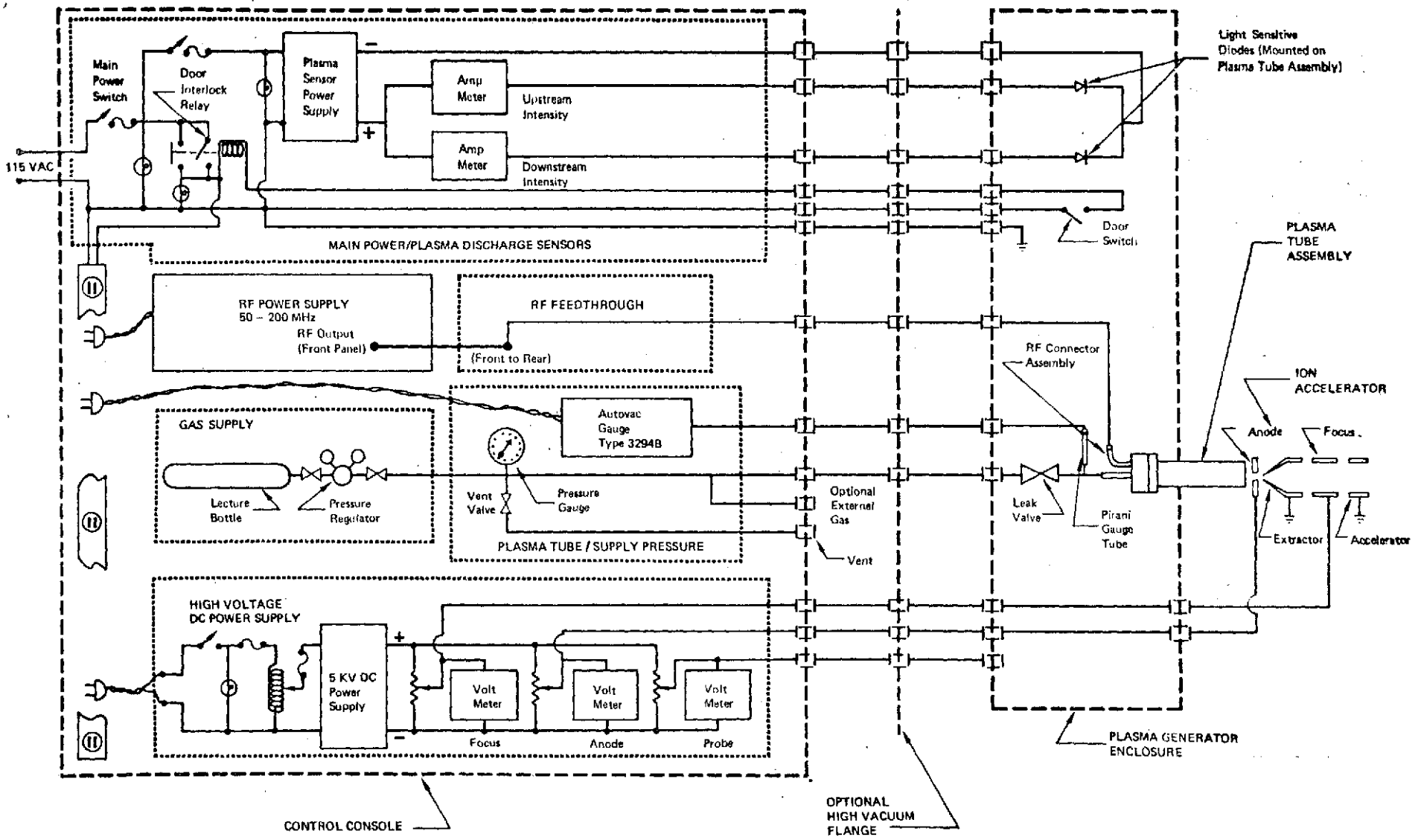

Figure 19: Act Device LDM General Gas/Electrical Diagram

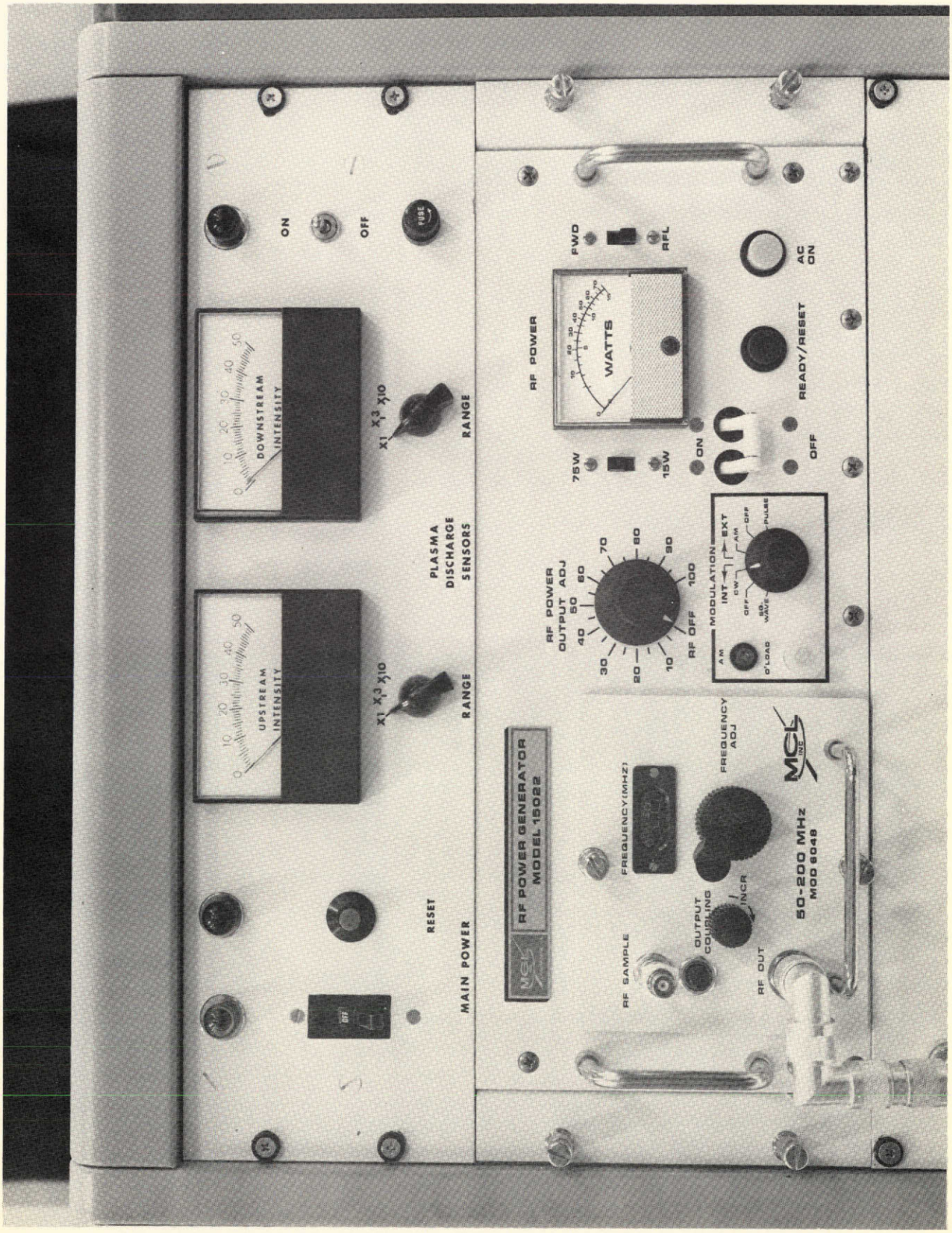

Figure 20: MAIN POWER/PLASMA DISCHARGE SENSORS PANEL AND RF POWER GENERATOR

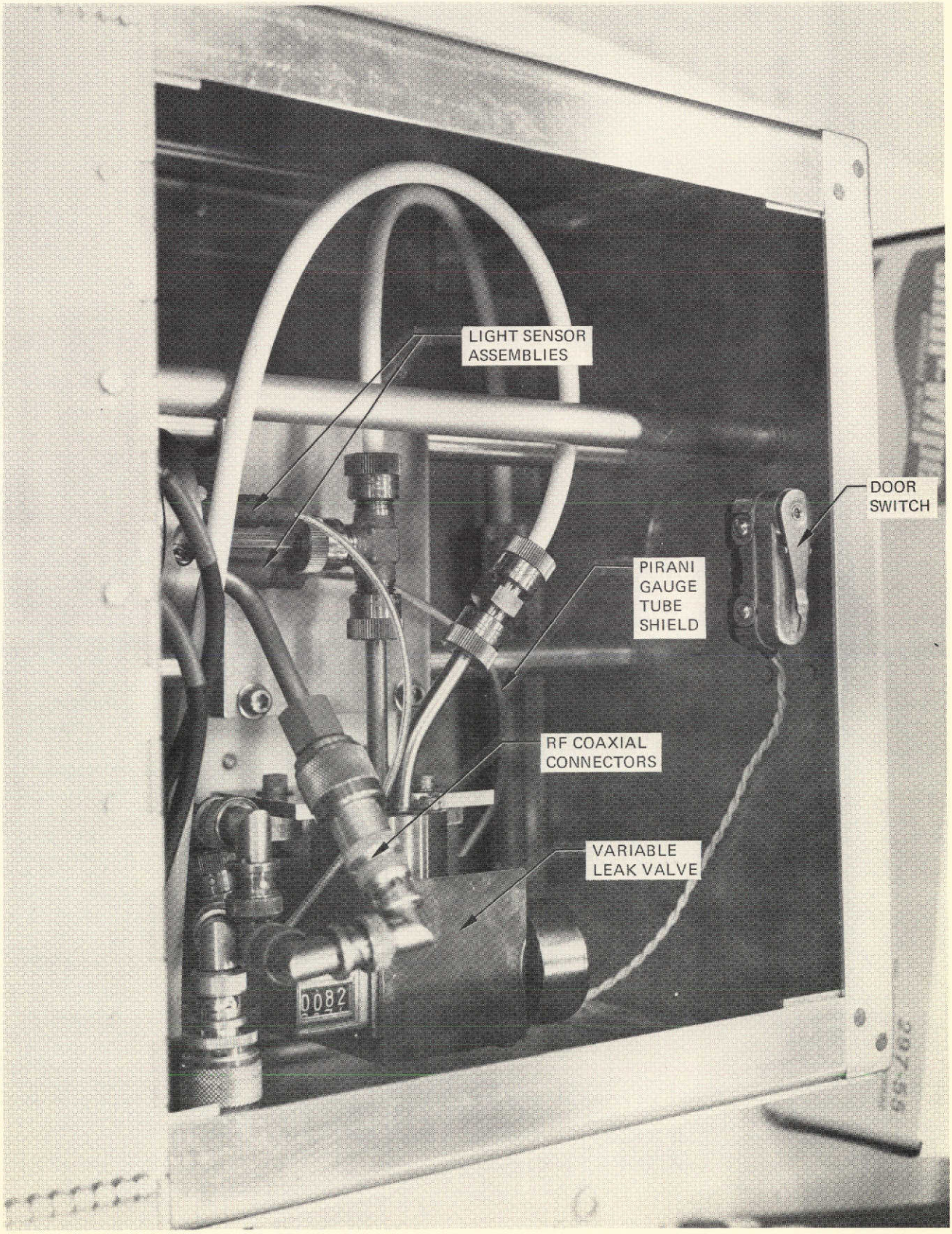

Figure 21: PLASMA GENERATOR ENCLOSURE INTERIOR

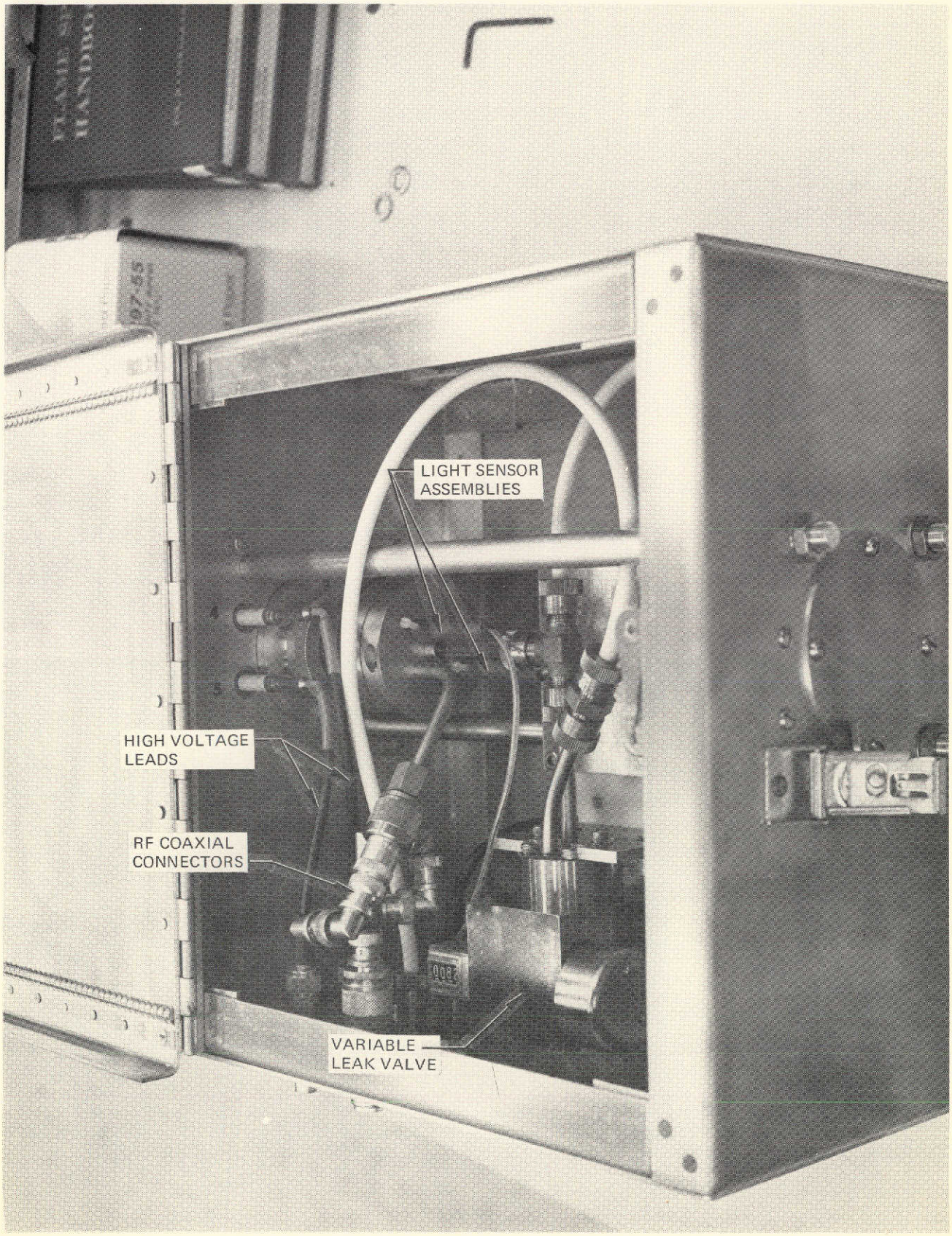

Figure 22: PLASMA GENERATOR ENCLOSURE INTERIOR

A minor modification of this unit was made to adapt it for use with the LDM. As delivered, the power generator has a protection circuit that turns off the power when the reflected (RFL) power exceeds a pre-set level (nominally 10 watts but re-set to 15 watts). To ensure initiation of the plasma discharge, an override circuit was installed which can be used to temporarily reduce the 'apparent' RFL power by a factor of 2.5. This override circuit is activated by the momentary contact switch labeled 'RFL/2.5' (see Figure 20).

The RF power output from the front of the generator is routed through the next lower panel to the rear of the control console. The RF power connection to the plasma tube assembly can be seen in Figure 21 and 22. Six coaxial 90° elbows are used to provide an adjustable coupling between the enclosure fitting and the plasma tube assembly.

4.4 Gas Supply System

The general diagram of the gas supply system is shown in Figure 19. For normal operation the gas is supplied from a lecture bottle, with pressure regulator, located in the control console. This gas supply panel is shown in the lower part of Figure 23. The pressure regulator controls the pressure supplied to the variable leak valve located inside the plasma generator enclosure. This leak valve may be seen in Figures 21 and 22. The combination of gas-supply pressure and leak-valve setting controls the gas flow rate through the plasma tube. This flow rate is related to the upstream plasma tube pressure which is measured with a Pirani gauge tube. The Pirani gauge tube installation is shown in Figure 21. A grounded RF shield protects the tube from burn-out. The gas supply pressure gauge and the Pirani gauge readout (AUTOVAC GAUGE type 3294B) of the plasma tube pressure are contained in the control console panel above the gas supply (see Figure 23). This panel also contains the vent valve which connects to a vacuum pumping system so that the system may be pumped and purged. An external gas supply connection is provided in case an external gas source is used. This connection is normally plugged.

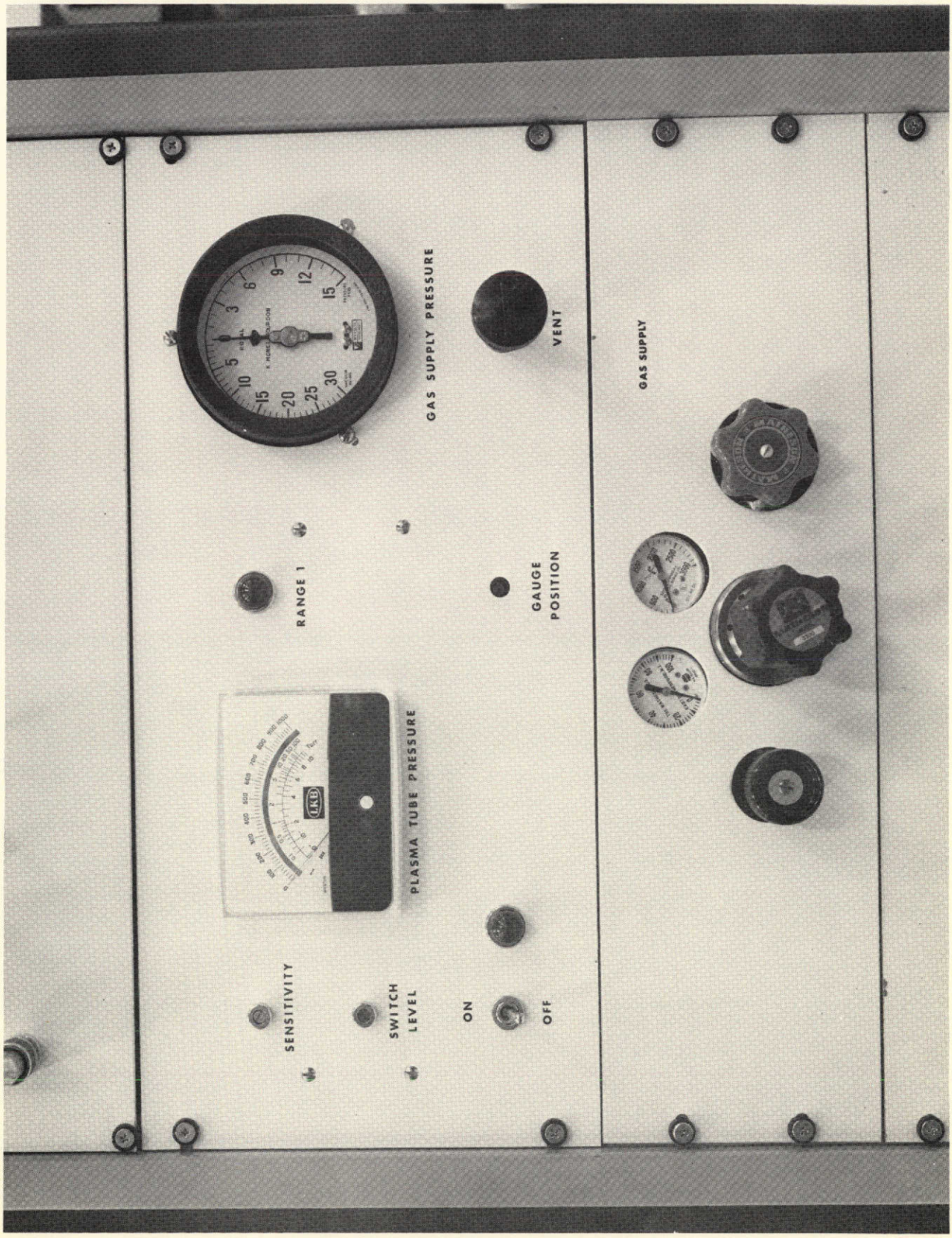

Figure 23: Gas Supply System Panels

4.5 Ion Accelerator System

The ion accelerator is a Gap-Einzel lens assembly which mounts as a unit to the plasma generator enclosure (see Figure 17). The basic accelerator lens design is identical to that developed in the design study phase (Reference 8). A high positive voltage on the anode extracts the electrons from the plasma and the ions are accelerated through the grounded extractor (see Figure 19). The ions are decelerated and focused as they pass through the focus lens which is at a high positive voltage. Finally the ion beam is accelerated out of the lens system by the grounded accelerator lens.

The high voltage DC power supply for the ion accelerator is located in the control console. Figure 24 shows a closeup view of this power supply panel. The power supply design was based on the design study results reported in Reference 8. Figure 19 shows that the high voltage is provided by a single 5 KV DC power supply and three sets of voltage dividers which allow fine voltage control for focus, anode and probe. The overall voltage level is set by the variac control of the power supply. Tests of the LDM showed that the probe (this probe is discussed in Reference 8) was not required for proper operation of the ion accelerator. Consequently no connections are made to this lead inside the plasma generator enclosure.

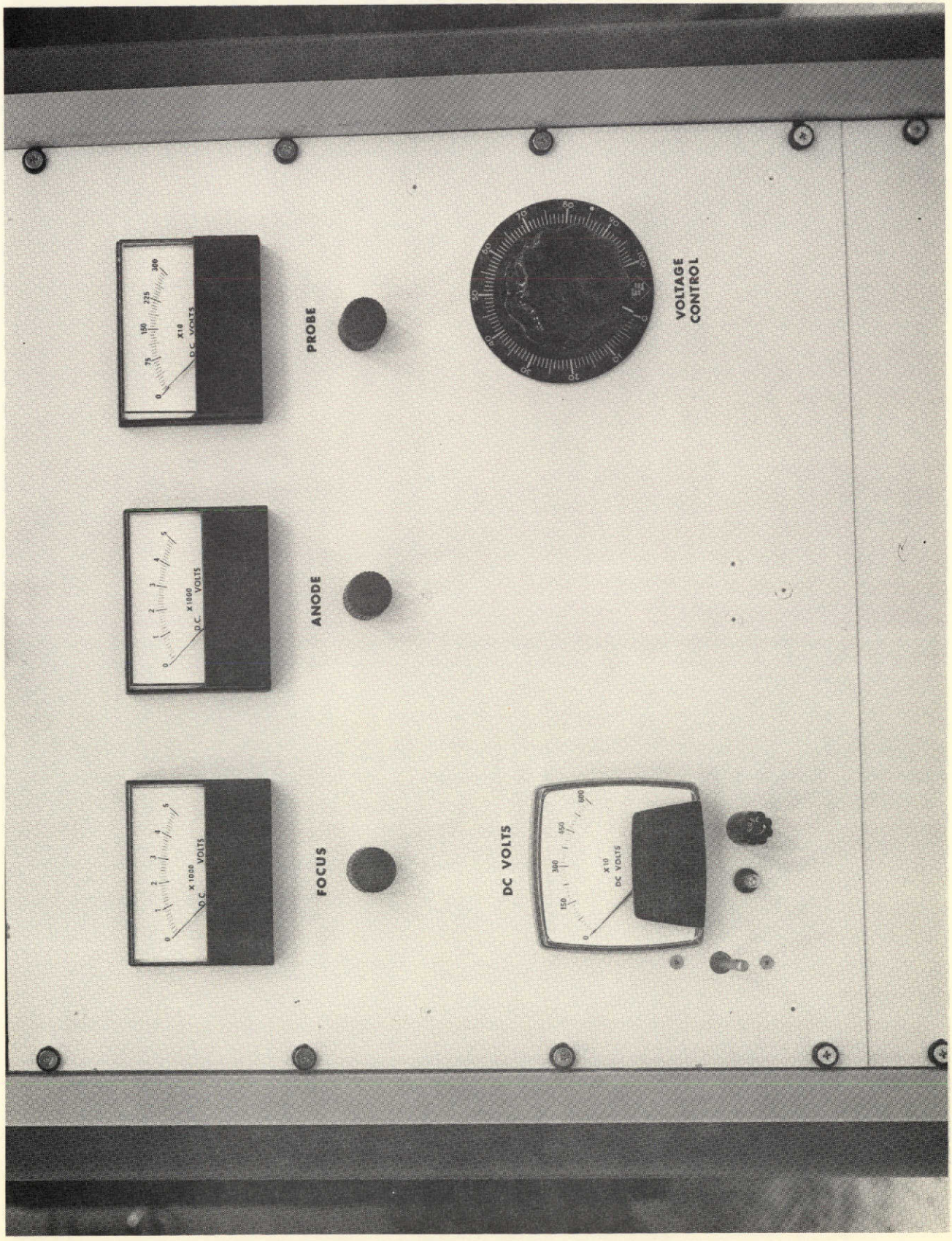

Figure 24: HIGH VOLTAGE POWER SUPPLY

5.0 PERFORMANCE TESTS

5.1 Gas Flow Rate Calibration

The LDM ACT device was delivered with one Pirani gauge tube installed in the plasma generator enclosure, and with two spare tubes. The installed tube is labeled as '4-ohm' and the spare tubes as '6-ohm'. A comparison of the pressure readouts on these tubes showed the 6-ohm tubes read about 15 percent higher than the 4-ohm tube.

The installed 4-ohm Pirani gauge tube was used to calibrate the oxygen flow rate as a function of plasma tube pressure. The calibration was accomplished by measuring the rate of pressure decay in a reservoir of known volume located upstream of the variable leak-valve. The plasma generator enclosure was mounted on a vacuum chamber in which the pressure was kept at about 10^{-5} torr during the measurements.

Figure 25 shows the results of this calibration along with the corrected calibration curve for use with the 6-ohm Pirani gauge tubes. The theoretical oxygen flow rate curve is also shown in Figure 25. (The gas flow rate analysis is the same as that used in Reference 8.) The agreement between theoretical and experimental values is quite good.

5.2 Preliminary Tests

Preliminary tests were made to determine the general operational characteristics of the LDM. Figure 26 shows the control console and the plasma generator enclosure during testing. Figure 27 shows the visible plume produced by the plasma generator at high vacuum conditions.

These preliminary tests resulted in the following observations:

(1) An electrode spacing of about 0.5 inch (1.27 cm) and a spacing between the RF electrode and the end of the plasma tube of about 0.5 inch (1.27 cm), produced the brightest visible plume at the desired oxygen flow rate.

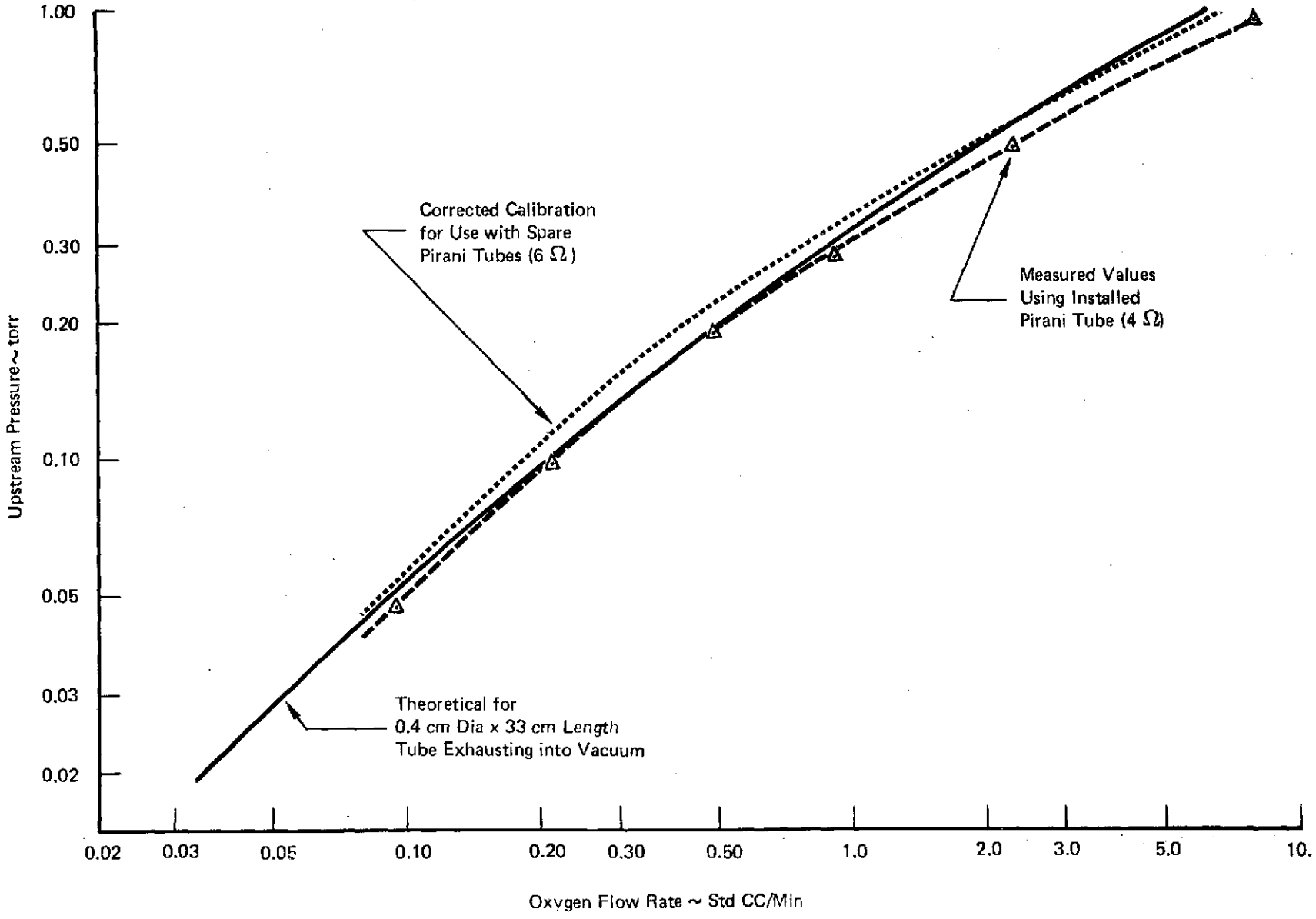

Figure 25: Plasma Tube Flow Rate Calibration

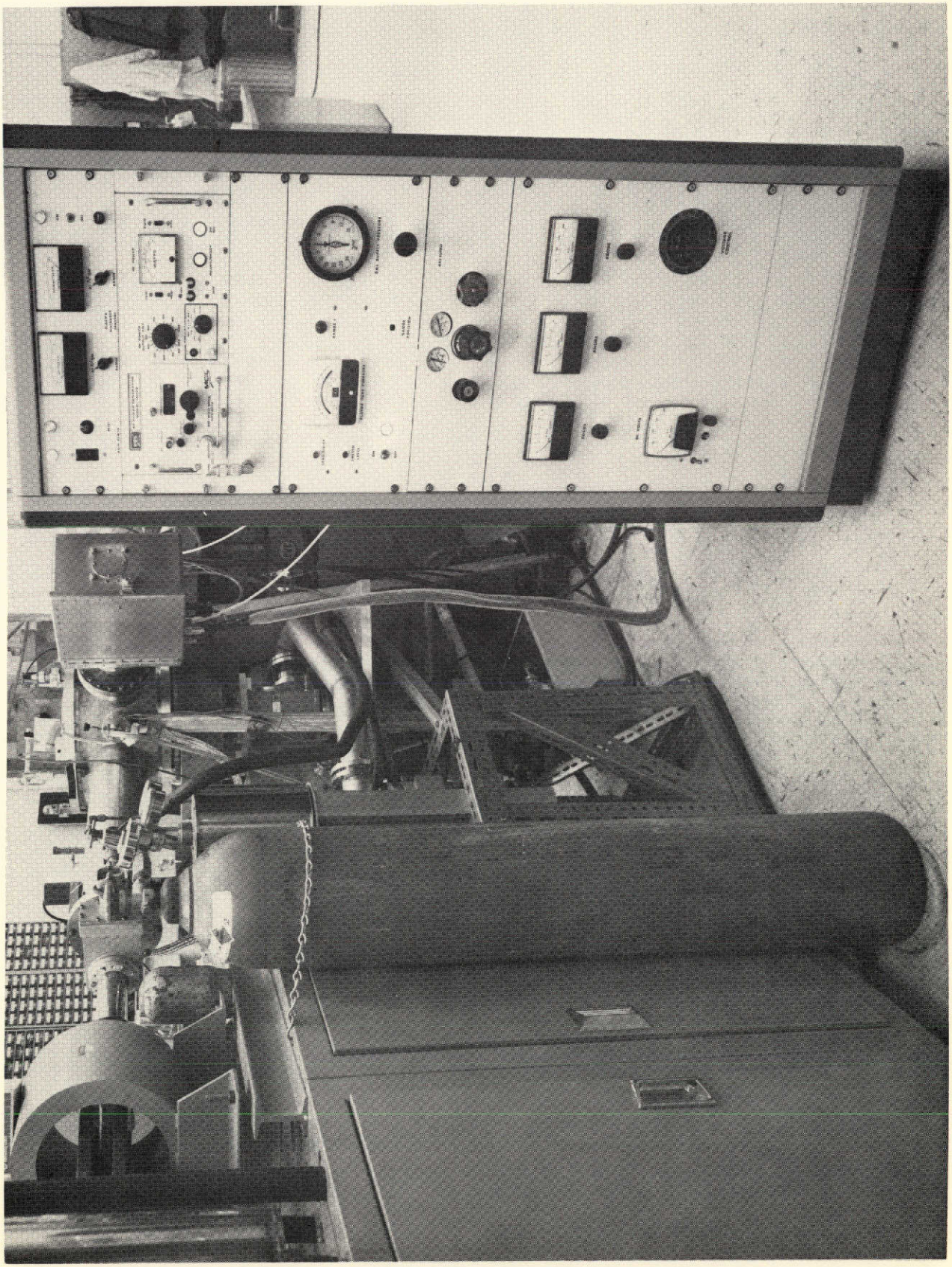

Figure 26: LDM ACT DEVICE DURING CHECKOUT TESTS

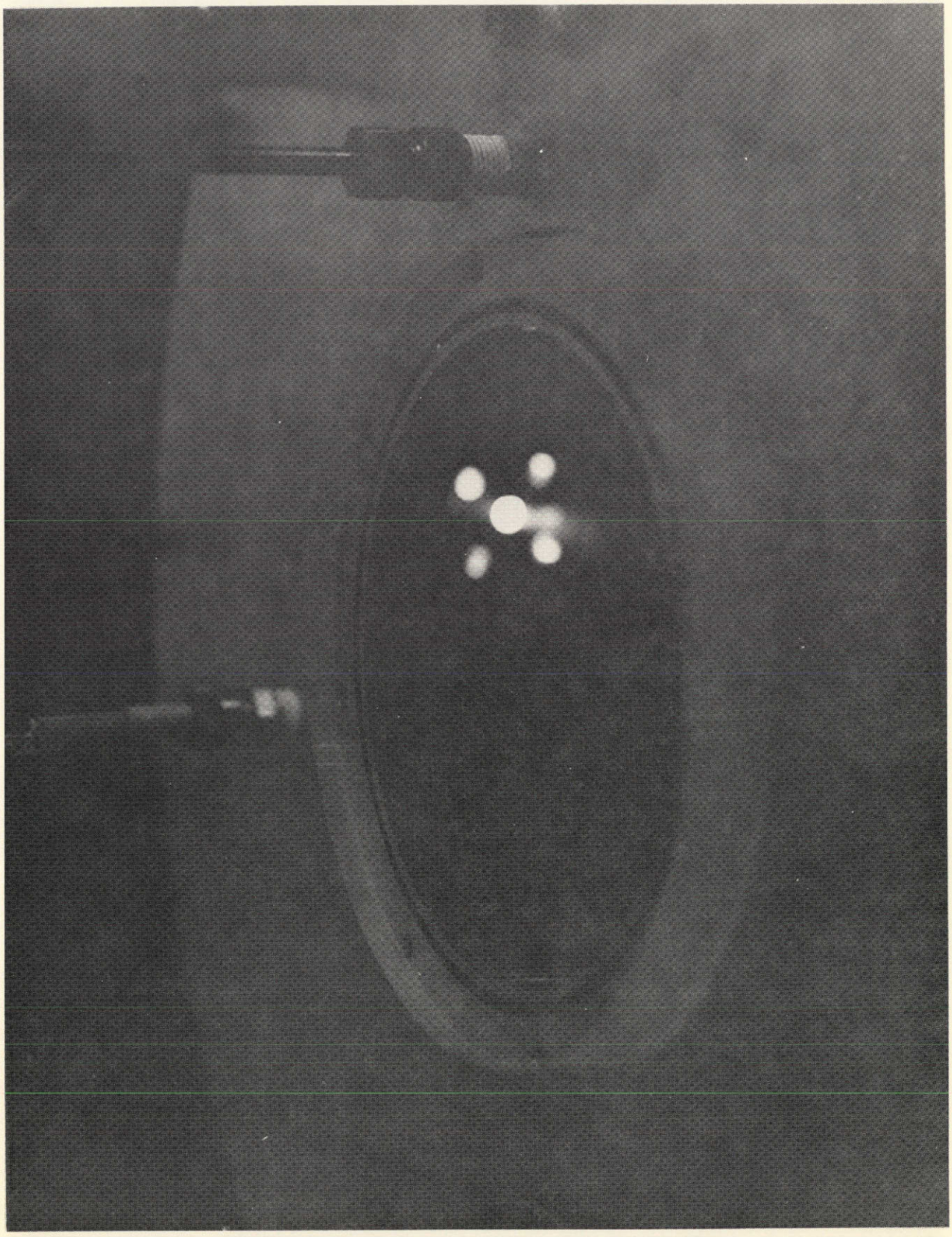

Figure 27: PLASMA TUBE OPERATION AT HIGH VACUUM

(2) The establishment and optimization of a visible plume could be correlated with the readings on the plasma discharge sensors. Figure 28 shows the correlation between downstream and upstream discharge intensity for proper operation.

(3) The initiation of the plasma discharge was difficult at times due to the protection circuit in the RF power generator which limited the maximum reflected power. This led to the installation of the override circuit discussed previously.

(4) With proper tuning of the RF power generator, the plasma discharge and visible plume could be maintained at power levels as low as 3 watts forward, and 1 watt reflected.

(5) The ion accelerator operated adequately without the added complexity of having a probe installed in the plasma tube.

5.3 Carbon Cleaning Tests

A carbon coated quartz-crystal-microbalance (QCM) was used to determine the carbon removal rate produced by the LDM ACT device. The QCM was mounted approximately on centerline 5 cm downstream of the plasma tube. The carbon removal rate was determined by measuring the rate of QCM frequency change for various oxygen flow rates and RF power levels. Table 1 presents the data taken during these tests. For the limited amount of data taken, the carbon removal rate appears to be primarily dependent on the forward RF power input. Figure 29 shows the correlation between carbon removal rate and forward RF power. The gas flow does not appear to have a significant effect on the cleaning rate. It was expected that the higher flow rates would provide a higher cleaning rate. This might still be the case if the plasma tube configuration be optimized for each flow rate.

5.4 Ion Accelerator Tests

A Faraday cup, mounted on centerline approximately 5-cm downstream of the accelerator, was used to measure the ion flux produced by the LDM ACT device. The ion current to the Faraday cup was measured for various oxygen flow rates, RF power levels, and accelerating voltages. During these tests the anode and focus voltages were set to the same level. In most cases only a slightly

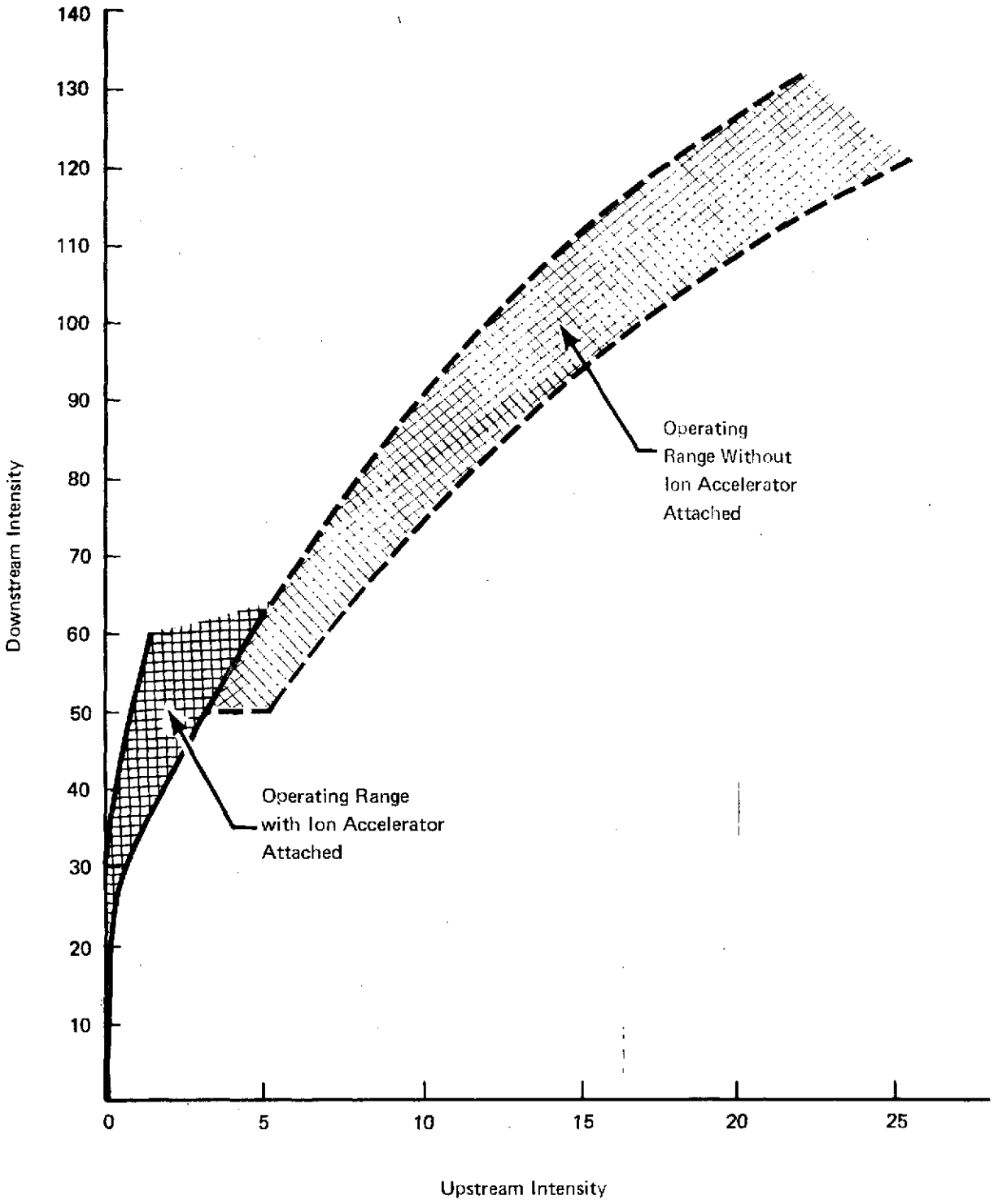

Figure 28: Proper LDM Operation Range

TABLE 1

CARBON CLEANING TESTS

PLASMA TUBE PRESSURE Torr	DISCHARGE INTENSITY UPSTREAM	DISCHARGE INTENSITY DOWNSTREAM	RF FREQUENCY Megahertz	RF POWER Watts FORWARD	RF POWER Watts REFLECTED	CARBON REMOVAL RATE *(QCM DATA) RATE OF FREQ. CHANGE Hz/Min	CARBON REMOVAL RATE *(QCM DATA) 10^{14} Atoms/ cm^2 - sec.
0.050	3	50	84	6	2	4.80	0.80
0.075	4	50	86	6	2	3.67	0.61
	10	90	86	12	5	9.0	1.50
0.075	20	120	86	15	7	10.2	1.70
0.10	3	50	84	4.5	1.6	2.53	0.42
	10	84	85	12	5	10.2	1.70
	26	120	86	15	7	7.2	1.20
0.10	23	130	83	19	7.5	13.0	2.18
0.20	7	50	83	6	1.8	1.0	0.17
0.20	14	90	83	18	5	6.33	1.06
0.075	18	120	84	14	5.8	10.7	1.79
0.075	14	78	80	15	0.5	8.15	1.36
0.050	5	50	84	13	3.5	9.88	1.65
0.030	4	50	84.5	13.5	5.5	16.5	2.76
0.015	3	50	85	15	7	5.47	0.92

*Carbon coated QCM centered about 5-cm from plasma tube

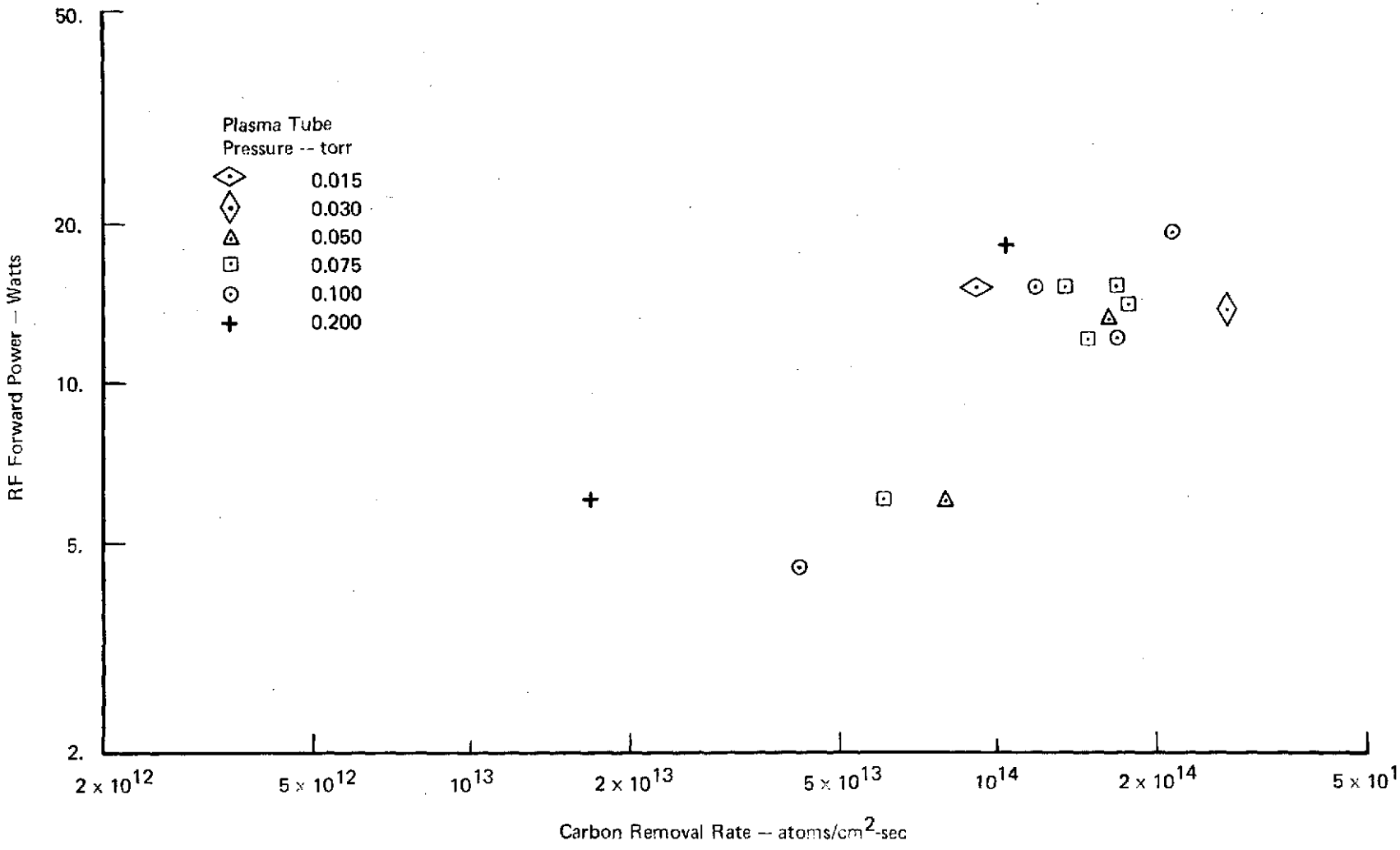

Figure 29: Rate of Carbon Removal - - 5 CM from Plasma Tube

larger ion flux could be achieved by optimizing the focus voltage for a given anode voltage. The data taken during these tests are given in Table 2. The maximum accelerating voltage that could be used was about 3KV. At higher voltages the plasma discharge was adversely affected and was sometimes extinguished. After attempts to operate at voltages higher than 3KV, the plasma discharge was difficult to reinitiate. The reason for this is not known.

As was the case for the carbon removal rate, the ion flux appears to be primarily dependent on the forward RF power input level. Figure 30 shows the correlation between ion flux and RF forward power. The ion flux is not greatly affected by either gas flow rate or accelerating voltage in the 1-3 KV range. At lower accelerating voltage the ion flux increases with increasing voltage.

TABLE 2

ION ACCELERATOR TESTS

PLASMA TUBE PRESSURE Torr	DISCHARGE INTENSITY		RF POWER Watts		RF FREQUENCY	ACCELERATOR VOLTAGE Kilovolts		*FARADAY CUP CURRENT 10^{-6} Amp
	UPSTREAM	DOWNSTREAM	FORWARD	REFLECTED	Megahertz	ANODE	FOCUS	
0.050	0	10	5.	1.5	81-83	1.	1.	0.25
	0	20	7.2	2.5				0.77
	0	30	11.5	4.1				0.94
	0.5	40	17.	5.4				1.07
	2.5	50	23.	7.5				1.15
	** 9.5	60	14	1.8		1.	1.	0.62
	0	10	5.5	2.		2.	2.	0.60
	0	20	10.0	3.8				0.85
	0	30	14.5	5.8				1.33
	2	40	16.	5.				1.55
	3	45	20.					1.9
	** 10.5	60	12	1.7		2.	2.	0.64
	0	10	5.1	0.8		3.	3.	0.45
	0	20	7.5	2.5				0.87
	0.5	30	11.	4.				1.05
	1.	40	15.	5.8				1.25
	3	50	19.	6.4				1.03
	** 9.5	60	13	1.2		3.	3.	0.82
	0	10	5.2	1.8		0.5	0.5	0.27
	0	20	9.	3				0.35
	0	30	13.5	5				0.36
	1.5	40	17	5.5				0.36
	2.5	50	24	7.5				0.37
0.050	** 9.5	60	12	0.8	81-83	0.5	0.5	0.32

** Mode of discharge changed-power increase reduces ion current

* Faraday cup centered about 5-cm from accelerator

TABLE 2 (Continued)

PLASMA TUBE PRESSURE Torr	DISCHARGE INTENSITY UPSTREAM	DOWNSTREAM	RF POWER Watts FORWARD	REFLECTED	RF FREQUENCY Megahertz	ACCELERATOR VOLTAGE Kilovolts ANODE	FOCUS	*FARADAY CUP CURRENT 10^{-6} Amp
0.10	0	10	4.1	1.5	85	0.5	0.5	0.08
	0	20	5.	2.2				0.125
	0.5	30	5.8	2.9				0.22
	1	40	9.0	4.0				0.31
	1.8	50	10.2	4.8	85			0.29
	2.5	60	20	9.5	86	0.5	0.5	0.38
	0	10	4.0	1.6		1.0	1.0	0.16
	0	20	5.5	2.2				0.23
	0.5	30	6.5	2.9				0.29
	1.0	40	9.	4.				0.38
	1.5	50	11.6	5.4				0.70
	2.5	60	21.	9.5		1.0	1.0	1.15
	0	10	3.5	1.5		2.0	2.0	0.17
	0	20	5	2				0.29
	.5	30	6.5	2.8				0.44
	1.0	40	8.5	3.8				0.60
	1.5	50	12.	5.5				0.82
	2.5	60	25.	11.3	86	2.0	2.0	1.88
	0	10	4.5	1.8	87	3.0	3.0	0.12
	0	20	6.0	2.2				0.22
	0.6	30	7.2	3.2				0.36
	1.2	40	9.4	4.2				0.54
	2.0	50	12.4	5.8				0.88
0.10	3.2	60	20	9.6	87	3.0	3.0	1.30
0.030	0	10	7	3	88	2	2	0.71
	0	20	10	4.5				0.93
	0	30	16	7				1.30
0.030	0.5	40	27	12.				1.92
0.020	0	10	8.5	3.9				0.56
	0	20	10	3.5				0.72
	0.8	30	12.5	5				0.56
	1.2	40	18	7.2				0.99
0.020	2.	50	28	11	88	2	2	1.50

TABLE 2 (Continued)

PLASMA TUBE PRESSURE Torr	DISCHARGE INTENSITY UPSTREAM	DOWNSTREAM	RF POWER Watts FORWARD	REFLECTED	RF FREQUENCY Megahertz	ACCELERATOR VOLTAGE Kilovolts ANODE	FOCUS	*FARADAY CUP CURRENT 10^{-6} Amp
0.075	0	10	5	2	81-83	0.5	0.5	0.12
	0	20	7.1	4				0.28
	0	30	16.	7.5				0.36
	0.5	40	23	11	81-83			0.37
	1.	50	19	8.2	86			0.40
	1.5	60	22	11	88	0.5	0.5	0.40
	0	10	4	1.5	85	1.	1.	0.22
	0	20	5.9	2.2				0.28
	0.5	30	8	3.5				0.48
	0.8	40	12.	5.1				0.85
	1.	50	17.	7.8				1.05
	2.	60	24	9.8		1.	1.	1.27
	0	10	3.5	1.2		2.	2.	0.22
	0	20	5	1.9				0.38
	0.5	30	7.1	3.				0.60
	1.0	40	10.2	4.5				0.77
	1.5	50	13	6.2				1.00
	3.8	60	20	8.5				1.45
	11.	90	27.	11.		2.	2.	3.2
	0	10	6.2	2.3		3.	3.	0.15
	0	20	8.5	3.8				0.34
	0	30	12.2	5.8				0.64
	.5	40	19	8.5	85			0.94
0.075	1.	50	25	8.	86	3.	3.	1.10

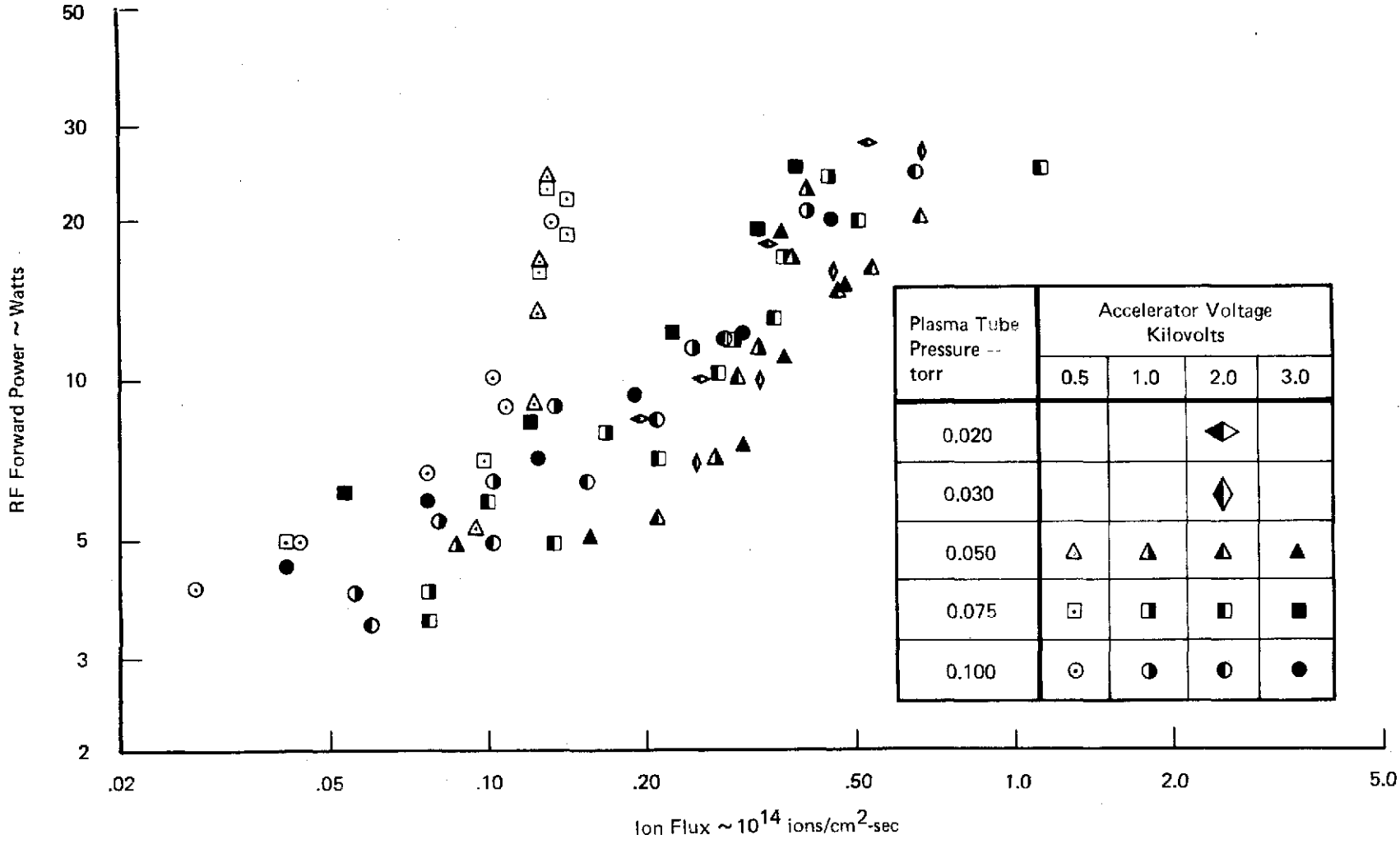

Figure 30: Ion Beam Flux - 5 cm From Accelerator

6.0 CONCLUSIONS AND RECOMMENDATIONS

A laboratory demonstration model ACT device has been developed for use at high vacuum ($<10^{-5}$ torr) conditions. This device operates in either a plasma cleaning mode or an ion sputtering mode. A control console and cable bundle allows the device to be operated at distance of up to 12 feet (3.66 m) from the vacuum chamber installation. The plasma generator enclosure can be either hard mounted on a vacuum chamber port or mounted inside a vacuum chamber. An additional cable bundle and vacuum flange feedthrough allows this inside chamber mounting at distances of up to 12 feet (3.66 m) from the vacuum feedthrough port.

The ACT device can be operated at gas flow rates of 0.03 to 0.5 std cc/min and RF power input levels of 5 to 25 watts. In the ion sputtering mode of operation the accelerating voltage can be varied from 1 to 3 KV. Tests in the plasma cleaning mode show that vacuum deposited carbon can be removed from a surface 5 cm away at rates of 5×10^{13} to 3×10^{14} atoms/cm^2-sec. The cleaning rate is primarily dependent on the RF power input to the plasma generator. Tests in the ion sputtering mode show that ion fluxes of 10^{13} to 10^{14} ions/cm^2-sec are achieved, 5 cm away from the accelerator, with accelerating voltage between 1 and 3KV. The ion flux is primarily dependent of the RF power input to the plasma generator.

An operational manual (Reference 9) has been prepared for the laboratory demonstration model ACT device. This manual provides: a detailed description of the device; operational procedures; assembly, installation and adjustment procedures; and a complete parts list. A complete set of engineering drawings has also been prepared.

In addition to demonstrating the plasma cleaning phenomena investigated under Contract NAS8-26385 (References 6 and 7), the device can serve as a useful tool for further investigation of plasma cleaning and ion sputtering. The device also establishes a base for further hardware development related to space flight or vacuum chamber uses.

It is recommended that further research, development, and applications studies be made on the ACT device. Further research is required to determine the plasma species responsible for cleaning and to determine the plasma cleaning mechanism. This determination could provide an explanation of the overcleaning effect noted in earlier studies, show the limitations on the type of contaminants that can be removed; and possibly provide guidelines as to the type of gas and operational mode required for different contaminants. This research would probably be general and long-termed involving basic considerations of the interaction between excited atoms and/or ions and the contaminant film. More specific and shorter-term research could be conducted to further investigate plasma exposure effects on silicon contaminants and typical spacecraft white paints.

Further development of the ACT device is also needed to complete its characterization and optimization. For example, a more complete characterization of the cleaning rate as a function of operating parameters is needed, and means of achieving the optimal plasma discharge mode need to be determined.

The capabilities of the LDM ACT device may have significant use in commercial applications. Appropriate commercial-application experiments need to be defined and conducted. This would allow the commercial applications of the plasma cleaning technique to be determined.

7.0 REFERENCES

1. Naumann, R., W. Moore, P. Nisen, W. Russell, and P. Tashbar, "Quartz Crystal Microbalance Contamination Monitors on Skylab - A Quick-Look Analysis," NASA TMX-64778, June 1973, George C. Marshall Space Flight Center, Marshall Space Flight Center, Alabama.

2. McKeown, D. and W. E. Corbin: "Removal of Surface Contamination by Plasma Sputtering," AIAA Paper No. 71-475 presented at 6th Thermophysics Conference, Tullahoma, Tennessee, April 1971.

3. Cothran, C. A., M. McCargo and S. A. Greenberg: "A Survey of Contamination of Spacecraft Surfaces," AIAA Paper No. 71-457 presented at 6th Thermophysics Conference, Tullahoma, Tennessee, April 1971.

4. Private Communication with Dr. G. Timothy, Harvard College Observatory, Cambridge, Massachusetts, April 1971.

5. Gillette, R. B. and B. A. Kenyon: Applied Optics 10, 3 (1971).

6. Gillette, R. B., W. D. Beverly and G. A. Cruz: "Active Cleaning Technique for Removing Contamination from Optical Surfaces in Space," Annual Report No. 1, Contract NAS8-26385, D180-14971-1, March 1972, The Boeing Company, Seattle, Washington.

7. Shannon, R. L., R. B. Gillette and G. A. Cruz: "Active Cleaning Technique for Removing Contamination from Surfaces in Space," Final Report, Contract NAS8-26385, D180-17610-1, August 1973, The Boeing Company, Seattle, Washington.

8. Shannon, R. L. and R. B. Gillette: "Active Cleaning Technique Device - Design Study Summary Report," Contract NAS8-28279, D180-15454-1, March 1973, The Boeing Company, Seattle, Washington.

9. Shannon, R. L: "Operation Manual for Laboratory Demonstration Model Active Cleaning Technique Device," Contract NAS8-28270, D180-18030-1, March 1974, The Boeing Company, Seattle, Washington.